The Effect of Synthetic Liquid Crystals on Amphotericin B Antifungal Activities

Sorakom Watcharapinchai

A Thesis Submitted in Partial Fulfillment of the Requirements for the Degree of

Master of Pharmacy in Pharmaceutical Sciences

Prince of Songkla University

2008

Thesis Title	The Effect of Synthetic Liquid Crystals on Amphotericin B Antifungal Activities
Author	Mr. Sorakom Watcharapinchai
Major Program	Pharmaceutical Sciences

Major Advisor

...……

(Assoc. Prof. Dr. Teerapol Srichana)

Examining Committee:

…….Chairperson

(Asst. Prof. Dr. Sanae Kaewnopparat)

…….Committee

(Assoc. Prof. Dr. Teerapol Srichana)

…….Committee

(Dr. Luelak Lomlim)

…….Committee

(Dr. Jiraporn Chingunpitak)

The Graduate School, Prince of Songkla University, has approved this thesis as partial fulfillment of the requirements for the Master of Pharmacy Degree in Pharmaceutical Sciences

……

(Assoc. Prof. Dr. Krerkchai Thongnoo)

Dean of Graduate School

ชื่อวิทยานิพนธ์ ผลของผลึกเหลวสังเคราะห์ต่อฤทธิ์การต้านเชื้อราของแอมโฟเทอริซิน บี

ผู้เขียน นาย สรคมน์ วัชราภินชัย

สาขาวิชา เภสัชศาสตร์

ปีการศึกษา 2551

บทคัดย่อ

แอมโฟเทอริซิน บี เป็นยากลุ่ม polyenes ที่ใช้ในการรักษาโรคติดเชื้อราในปอดมานานกว่า 30 ปี เป็นยาที่มีประสิทธิภาพสูง และใช้เป็นยาอันดับแรก ในการรักษาผู้ป่วยที่ติดเชื้อรา โดยรูปแบบยาเตรียมของยา แอมโฟเทอริซิน บี ที่ใช้อยู่ในปัจจุบันแบ่งออกเป็น 2 รูปแบบใหญ่ๆ คือยาในรูปแบบ Conventional amphotericin B โดยใช้ sodium deoxycholate เป็นสารก่อไมเซลล์เพื่อเพิ่มค่าการละลาย ในชื่อการค้าคือ Fungizone ® แต่มีข้อเสีย คือทำให้เกิดอาการข้างเคียงจากการใช้ยาสูง เช่น อาการไข้ หนาวสั่น เม็ดเลือดแดงแตก และอีกรูปแบบเป็นยา amphotericin B lipid complex ได้แก่ Ambisome ®, Amphotec ® และ Abelcet® ยารูปแบบดังกล่าวต้องใช้ขนาดยาที่สูงกว่า conventional amphotericin B ซึ่งการใช้ยาขนาดที่สูงอาจทำให้เกิดการสะสม และเกิดพิษจากการใช้ยาได้

ในการศึกษานี้ได้นำผลึกเหลวสังเคราะห์มาเป็นแนวทางใหม่ในการนำส่งยาแอมโฟเทอริซิน บี เพื่อลดความเป็นพิษและเพิ่มความคงตัวของยาแอมโฟเทอริซิน บี วัตถุประสงค์ในการศึกษาครั้งนี้คือการสังเคราะห์ผลึกเหลว cholate cetyl ether (CCE) และนำไปวิเคราะห์โครงสร้างด้วย fourier transformed infrared spectroscopy, mass spectrometry and nuclear magnetic resonance spectroscopy พบว่า สูตรโมเลกุลของสารเป็น $C_{40}H_{69}O_4$ ซึ่งประกอบไปด้วย 3 ส่วนคือ ส่วนที่

เป็นสเตียรอยด์ สายไฮโดรคาร์บอน และ พันธะอีเทอร์ที่เชื่อมระหว่างโครงสร้างทั้ง 2 ส่วน และพบว่าโครงสร้างของ CCE เกิดผ่าน intermediate ของ cholesteryl cetyl carbonate ester (CCC) โดยการสูญเสียคาร์บอนไดออกไซด์จากโมเลกุลที่อุณหภูมิห้อง ผลของการศึกษาจาก differential scanning calorimetry และ X-ray diffraction พบว่าสารเป็นอสัณฐานที่อุณหภูมิห้อง จากการศึกษาความคงตัวของยาแอมโฟเทอริซิน บี ในผลึกเหลวพบว่า ยาแอมโฟเทอริซิน บี ถูกบรรจุเข้าไปใน CCE อย่างสมบูรณ์ ทำให้ระบบมีขนาดอนุภาค 243 ± 48 นาโนเมตร และพบว่า แอมโฟเทอริซิน บี ใน CCE สามารถรักษาความเป็น monomer ของยา ตลอดการเก็บรักษาเป็นเวลา 14 วัน ในการทดสอบความไวและความแรงของยาแอมโฟเทอริซิน บี ใน CCE โดยวิธี cylinder-plate และ broth micro dilution พบว่า CCE สามารถเสริมการออกฤทธิ์ของยาแอมโฟเทอริซิน บี โดยให้ค่าการยับยั้งของเชื้อราที่ต่ำกว่ายาแอมโฟเทอริซิน บี บริสุทธิ์ จากการทดสอบความเป็นพิษของยาแอมโฟเทอริซิน บี ใน CCE พบว่าไม่เป็นพิษกับเม็ดเลือดแดงที่ความเข้มข้นยา 1 ไมโครกรัมต่อมิลลิลิตรและไม่เป็นพิษต่อเซลล์ monocyte และ macrophage ที่ความเข้มข้นยา 10 ไมโครกรัมต่อมิลลิลิตรจากผลการทดลองข้างต้น สรุปว่า CCE มีศักยภาพที่จะใช้ในระบบการนำส่งยาแอมโฟเทอริซิน บีได้

Thesis title	The effect of synthetic liquid crystals on amphotericin B antifungal activities
Author	Mr.Sorakom Watcharapinchai
Major Program	Pharmaceutical Sciences
Academic year	2008

ABSTRACT

Amphotericin B (AmB) is a polyene drug which has a high efficacy in the treatment of systemic fungal infections for 30 years. There are two dosage forms of AmB available nowadays, the first dosage forms is called conventional dosage formulations (Fungizone®). Sodium deoxycholate was used as a micelle forming agent to increase solubility of AmB. However, it has a serious side effect such as chill, fever, hemolysis and nephrotoxicity. Later, liposomes encapsulated AmB were developed to overcome the side effects from conventional AmB. It was called Amphotericin B lipid complex which are Ambisome®, Amphotec® and Abelcet®. The recommended doses of lipid formulation are higher than those of conventional AmB. Free AmB from liposome may be accumulated in the organ and lead to toxicity.

In this study, the synthetic liquid crystal was introduced as a new approach in the design of novel nanosystems of AmB. It was aimed that the liquid crystal should decrease AmB toxicity and increase stability of AmB. The objectives were to synthesize cholate cetyl ether (CCE). CCE was characterized by fourier transformed infrared spectroscopy, mass spectrometry and nuclear

magnetic resonance spectroscopy. It is evident that the molecular formula was $C_{40}H_{69}O_4$ and CCE structure contains three parts; a steroid nucleus, one hydrocarbon chains, and ether linkage between both parts. The CCE structure was rearranged from cholesteryl cetyl carbonate ester (CCC) by the loss of carbon dioxide room temperature. According to differential scanning calorimetry and X-ray diffraction, CCE was amorphous at room temperature. It was shown that AmB was completely loaded in CCE with a size of 243 ± 48 nm. Moreover, AmB-CCE was likely to be in a monomeric form during storage for 14 days. For the susceptibility test by cylinder plate and broth microdilution method, it was found that CCE enhanced the activity of AmB resulting in lower MICs than pure AmB. From the result of cytotoxicity test, the AmB-CCE nanosystem was not toxic to RBC at AmB 1 μg/ml and also not toxic to monocyte and macrophage cell line at 10 μg/ml. CCE seems to give a promising result in using as nanomaterial in AmB formulations.

ACKNOWLEDGEMENT

The finish of my thesis involves efforts of many dedicated people. First of all, I would like to express my sincere gratitude and deep appreciation to my advisor, Associate Professor Dr. Teerapol Srichana for all of the valuable advice, guidance, encouragement and help throughout my writing up.

My gratitude goes to our colleagues at Department of Pharmaceutical Technology, Faculty of Pharmaceutical Sciences, Prince of Songkla University for all the support provided during my master's program. I have taken advantage of the generosity of too many of them who I cannot name individually, but I would like to thank to all staff of Faculty of Pharmaceutical Sciences for their contributions throughout this study.

My special appreciation goes to the Department of Microbiology, Faculty of Sciences and the staff for giving me the opportunity to use their equipment and facilities. Special thanks go to Assistant Professor Dr Athip Nilkaew, who allowed me to use the ultracentrifugation. This study could not have been completed without biological samples from the Department of Pathology, Faculty of Medicine.

I would like to give special thank to the Drug Delivery System Research Center and National Nanotechnology Center for the funding to present at 2nd IEEE International Nanoelectronics 2008 Conference in conjunction with Shanghai , Nanophotonics and Electronics forum, Shanghai, China.

My deep appreciation goes to the staff in the Scientific Equipment Center and Scientific Equipment Center for their analytical equipment and advices.

I am gratefully to give special thanks to PhD students (Ms Rabkwan Chualee and Ms. Narumon Changsan) and Master Degree student (Ms. Nanchanit Aeinleng) for constructive advice. Finally, great respect goes to my beloved parent and I would like to give my special thanks to my friends for their generous kindness and our togetherness in all situations through our long friendship.

Sorakom Watcharapinchai

CONTENTS

	Page
CONTENTS	**vi**
LIST OF TABLES	**xvi**
LIST OF FIGURES	**xvii**
LIST OF ABBREVIATIONS AND SYMBOLS	**xx**
CHAPTER	
1. INTRODUCTION	
1.1 Background, Rationale and Objective	1
1.2 The problem of AmB	
1.2.1 Unstability of AmB	3
1.2.2 Nephrotoxicity	6
1.2.3 Hemolysis	6
1.2.4 Cost of AmB	8
1.3 Proposed research	9
1.4 Objectives of thesis	12
2. REVIEW OF LITERATURES	
2.1 Fungal cell structure and targets	13

CONTENTS (CONT.)

	Page
2.2 Molecular basis of sterol specificity of polyene	13
2.3 Effect of AmB with oxidation dependent events in stimulatory lethal effect	18
2.4 AmB against *C. neoformans*	18
2.5 Research and development of AmB	
2.5.1 Conventional AmB	19
2.5.2 Lipid formulations of AmB	
2.5.2.1 Liposomal AmB (LAmB) or Ambisome	21
2.5.2.2 AmB lipid complex (ABLC)	22
2.5.2.3 AmB colloidal dispersion (ABCD)	22
2.6 Liquid crystal and research development	
2.6.1 Definition	24
2.6.2 Type of the liquid crystal	
2.6.2.1 Thermotropic liquid crystal	26
2.6.2.2 The lyotropic liquid crystal	28
2.7 Pharmaceutical research development in liquid crystal	30

CONTENTS (CONT.)

Page

3. MATERIAL AND METHOD

3.1 Synthesis and characterization of CCE

3.1.1 Synthesis of CCE 33

3.1.2 Characterization of purified CCE

3.1.2.1 Fourier transform infrared spectroscopy (FTIR) 36

3.1.2.2 NMR spectroscopy (^{13}C-NMR, ^{1}H-NMR) 37

3.1.3.3 Electrospray ionization mass spectrometry (ESI-MS) 37

3.1.2.4 Differential scanning calorimetry (DSC) 37

3.1.2.5 X-ray diffractometer (XRD) 38

3.2 Stability testing of pure AmB and AmB in liquid crystal

3.2 1 HPLC of AmB in liquid crytsal

3.2.1.1 Preparation of standard solutions and AmB in liquid crystal 39

3.2.1.2 Chromatographic system and conditions 39

3.2.2 Content of AmB in liquid crystal 40

3.2.3 Chemical stability of pure AmB and AmB in liquid crystal 40

3.2.4 Size stability of pure AmB and AmB in liquid crystal 41

CONTENTS (CONT.)

Page

3.3 Microbial assay of pure AmB and AmB in liquid crystal

3.3.1 Potency of pure AmB and AmB in liquid crystal

3.3.1.1 Preparation of inoculum and inoculated medium 42

3.3.1.2 Preparation of standard solution and sample solution 42

3.3.1.3 Preparation of buffer No.10 (0.2 M, pH 10.54) 43

3.3.1.4 Cylinder plate analysis 43

3.3.2 Susceptibilty test with *C. neoformans* by broth microdilution

3.3.2.1 Preparation of inoculum 44

3.3.2.2 Preparation of sample stock solution 45

3.3.2.3 Broth microdilution analysis 45

3.4 Cytotoxicity evaluation of pure AmB and AmB in liquid crystal

3.4.1 Hemolysis of pure AmB and AmB in liquid crystal

3.4.1.1 Hemolysis analysis 46

3.4.1.2 Preparation of phosphate buffer saline (PBS) pH 7.4 47

CONTENTS (CONT.)

Page

3.4.2 Cytotoxicity studies of pure AmB and AmB in liquid crystal with cell line

3.4.2.1 Preparation of cell line 47

3.4.2.2 Preparation of sample 48

3.4.2.3 Cytotoxicity determination of pure AmB, pure liquid crystal and AmB in liquid crystal 49

4. RESULTS AND DISCUSSION

4.1 Synthesis and characterization of CCE

4.1.1 Synthesis of CCE 50

4.1.2 Characterization of purified CCE 53

4.1.2.1 FTIR spectrum analysis 52

4.1.2.2 NMR spectrum analysis 53

4.1.3.3 ESI-MS analysis 56

4.1.2.4 DSC and XRD analysis 57

4.2 Stability testing of pure AmB and AmB in liquid crystal

4.2.1 HPLC of AmB in liquid crystal 58

4.2.2 Content of AmB in liquid crystal 59

CONTENTS (CONT.)

	Page
4.2.3 Chemical stability of pure AmB and AmB in liquid crystal	60
4.2.4 Size stability of zeta potential of pure AmB and AmB in liquid crystal	61
4.4 Microbial assay of pure AmB and AmB in liquid crystal	
4.4.1 Potency of AmB in liquid crystal	65
4.4.2 Susceptibility testing of *C. neoformans* by broth microdilution analysis	66
4.5 Cytotoxicity of pure AmB and AmB in liquid crystal	
4.5.1 Hemolysis of pure AmB and AmB in liquid crystal	68
4.5.2 Cytotoxicity of pure AmB and pure liquid crystal AmB in liquid crystal with monocyte and alveolar macrophage	70
5. CONCLUSIONS	75
BIBLIOGRAPHY	77
APPENDIX	84
VITAE	92

LIST OF TABLES

Table		Page
1.1	Average cost therapy of AmB in various formulations for one week	8
2.1	Composition and structure of lipid–based AmB formulations	23
4.1	^{13}C and ^{1}H resonance assignment of cholate cetyl ether (CCE) as compared with deoxycholic acid	55
4.2	Free AmB and AmB in different liquid crystals by HPLC	60
4.3	Zetapotential of pure AmB and AmB in liquid crystal	64
4.4	MICs of *C. neoformans* for pure AmB, pure liquid crystal and AmB in CCE by broth microdilution analysis	67

LISTS OF FIGURES

		Page
Figure 1.1	Structures of Amphotericin (A), Cholesterol (B), Ergosterol (C)	2
Figure 1.2	Aggregation structure of Linear aggregation (A), Cylinder aggregation (B)	4
Figure 1.3	The UV band absorption of AmB in aqueous medium, the monomeric form (A), the dimeric form after 5 days (B)	5
Figure 1.4	Time dependent hemolysis profile of AmB (~3 μg/ml) (▲), AmB-loading surfactant micelles formulations (□) and buffer (●)	7
Figure 1.5	The structures of cholate cetyl ether (CCE)	10
Figure 1.6	Design of ionophore of bile acid with acid with amine	10
Figure 1.7	Model structure of AmB in CCE nanosystem	11
Figure 2.1	Model structure of AmB-ergosterol channel.	14
Figure 2.2	Schematic representation of hydrogen bond formation	15
Figure 2.3	Mechanism of AmB on transmembrane pore in fungal cell	17
Figure 2.4	Formation mechanism of AmB-LDL receptor on the transmembrane pore with mammalian cells	17
Figure 2.5	Liposome AmB structure	21
Figure 2.6	AmB lipid complex (ABLC) structure	22

LISTS OF FIGURES (CONT.)

		Page
Figure 2.7	Arrangement of thermotropic liquid crystal	27
Figure 2.8	Changing of lyotropic liquid crystal formation above kraft temperature (T_k)	30
Figure 2.9	The structure of cholesteryl oleyl carbonate ester (COC)	31
Figure 3.1	The synthesis and rearrangememt of CCE structure	34
Figure 4.1	The structure of CCE	51
Figure 4.2	TLC of CCE mixture and starting materials	51
Figure 4.3	FTIR spectrum of CCE	53
Figure 4.4	^{13}C-NMR spectrum of CCE (A) and ^{1}H-NMR spectrum of CCE (B)	54
Figure 4.5	Mass spectrum of CCE	56
Figure 4.6	Fragmentation of hydrocarbon chain in CCE molecule	57
Figure 4.7	The cooling curve DSC thermogram of CCE	58
Figure 4.8	X-ray diffraction of CCE	58
Figure 4.9	HPLC chromatograms of free AmB standard analysis	59
Figure 4.10	UV spectrum of AmB 100 µg/ml (A), AmB-CCE, (B) AmB-COC (C) in aqueous solution during 14 days	63
Figure 4.11	Size stability of pure AmB 10 µg/ml in the aqueous solution (□), AmB-CCE (●) AmB-COC (▲) during 14 day	64

LISTS OF FIGURES (CONT.)

Page

Figure 4.12 Photographs of the zone diameter for AmB standard (A) and AmB in liquid crystal (B) 66

Figure 4.13 Concentration dependent and time hemolysis profile 69

Figure 4.14 RBC observed under light microscope at magnification 200 70

Figure 4.15 The % viability of monocyte J 774.2 cell line (◆) and macrophage NR 8383 cell line (○) after incubation with AmB (A), the % viability of monocyte J 774.2 cell line (B) and the % viability of macrophage NR 8383 cell line (C) after incubation in CCE (□), DCA (■) and COC (▲) 73

Figure 4.16 The % viability of monocyte J 774.2 cell line(A), macrophage NR 8383 cell line after incubation with AmB 100 µg/ml in CCE (□), DCA (■), COC (▲) (B) and the % viability of monocyte J 774.2 cell line (C), macrophage NR 8383 (D) cell line after incubation with AmB 10 µg/ml in CCE (□), DCA(■), COC (▲) 74

LISTS OF ABBREVIATIONS AND SYMBOLS

Symbols of Common Terms

$	=	American dollar
AmB	=	Amphotericin B
ABCD	=	AmB colloidal dispersion
ABLC	=	AmB lipid complex
Å	=	Angstorm
ATCC	=	American Type Culture Collection
^{o}C	=	Degree Celcius
CCC	=	Cholesteryl cetyl carbonate ester
COC	=	Cholesteryl oleyl carbonate ester
CCE	=	Cholate cetyl ether
CFU	=	Colony forming unit
cm	=	Centimeter
DCA	=	Deoxycholic acid
DMSO	=	Dimethyl sulphoxide
e.g.	=	For example
g	=	Gram
h	=	Hour

Symbols of Common Terms

HPLC	=	High performance liquid chromatography
kg	=	Kilogram
λ	=	Wavelength
T_k	=	Kraft temperature
L	=	Liter
LAmB	=	Liposomal AmB
LDL	=	Low density lipoprotein
µg	=	Microgram
µl	=	Microliter
µm	=	Micrometer
mg	=	Milligram
M	=	Molar
m/z	=	Mass divided by charge
MIC	=	Minimum Inhibitory Concentration
min	=	Minute
mmol	=	Millimole
ml	=	Milliliter

LISTS OF ABBREVIATIONS AND SYMBOLS (CONT.)

Symbols of Common Terms

mm	=	Millimeter
MW	=	Molecular Weight
N	=	Normality
n	=	Number of Sample
NCCLS	=	National Committee for Clinical Laboratory Standards
nm	=	Nanometer
%	=	Percentage
PBS	=	Phosphate-Buffered Saline
r^2	=	Correlation Coefficient
RBC	=	Red Blood Cell
rpm	=	Round Per Minute
sec	=	Second
sd	=	Standard Deviation
TMS	=	Tetramethylsilane
UK	=	United Kingdom
USA	=	The United States of America
USP	=	The United States Pharmacopeia

Symbols of Common Terms

UV	=	Ultraviolet
V	=	Volt
v/v	=	Volume by volume
w/v	=	Weight by volume

CHAPTER 1

INTRODUCTION

1.1 Background and Rationale

The incidence of deep-seated mycosis has increased especially in respiratory tract, problem due to an increased in the number of compromised hosts in patients with human immunodeficiency virus infection (Takakazu and Mohammad, 1998). This problem has grown more serious. Despite the introduction of new azole antifungal agents (fluconazole, itraconazole), amphotericin B (AmB) remains to be a drug of choice for the treatment of systemic fungal infections. It was the first antifungal drug commercially available in the market (Antoniadou and Dupont, 2005). AmB is one of the polyene macrolide antifungal drugs produced by South American soil bacterium *Streptomyces nodosus*. Powerful and broad spectrum fungicide owes its activity to a unique amphoteric molecular structure that allows it to concentrate in cell membrane (Bekersky *et al.,* 1999).

The AmB molecular mechanism of action has still not been understood well enough to make rational design of new derivatives. It has been known that AmB interacts with the component of cell membrane and forms ion channel (Baginski and Borowski, 2002). These ion channels disrupt membrane functions and cause uncontrolled cation transport (through increase in

cell membrane permeability) leads to the leakage of sodium, potassium and hydrogen ion, where it associates with membrane sterols to form pores which damage the cell ions, and eventual cell death. According to the widely accepted sterol hypothesis, the presence of sterol molecules in the membrane is necessary for AmB to be able to form conducting channels. Its primary mechanism of action is via binding to ergosterol, the most abundant sterol found in the cell membrane of sensitive fungi, and the creation of a barrel pore (Fournier *et al.,* 1998). The selective activity of AmB towards fungi cause by its higher affinity to ergosterol than cholesterol, the principal sterol in the fungal cells as shown in Figure 1.1 (Baginski *et al.,* 2002). AmB is active against *Aspergillus*, *Candida*, *Blastomyces*, *Coccidioides*, *Histoplasma*, *Sporothrix*, *Paracoccidioides*, *Cryptococcus*, and *Mucor* species. In addition, AmB provokes lipid peroxidation, immune stimulation especially monocyte and macrophage cell (Fournier et *al.,* 1998).

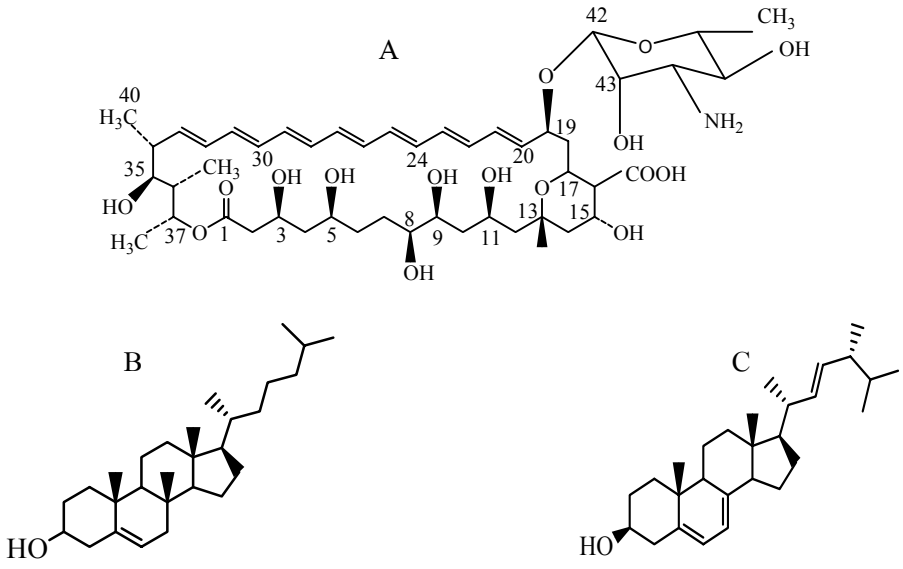

Figure 1.1 Structures of Amphotericin B (A), Cholesterol (B), Ergosterol (C)

1.2 The problem of AmB

1.2.1 Unstability of AmB

The AmB molecule consists of a large lactone ring, one side of which is a non polar conjugate heptene, while the other side is a polar hydroxyl group. The amino sugar mycosamine attaches to the macrolide ring by a glycosidic bond. Thus, AmB is amphiphillic. It is also hydrophilic, due to the presence of a carboxyl and amino groups which are charged at the physiological pH. These molecular characteristics stimulate AmB to form aggregates in aqueous media and decrease solubility.

In the structure proposed for two symmetric intermolecular hydrogen bonds between the 35-OH group of first molecule and O-42 group of second molecule are crucial for molecular arrangement of the dimer formation as shown in the Figure 1.1 A. The aggregation behaviour involves of the ionic state and netcharge of the AmB molecule. The first step aggregation was caused from the dimerization of monomers to more hydrophilic dimers. The particle size of aggregation of AmB in aqueous media contain many different species with a molecular weight in the range of one thousand (monomer) to a few million (colloid type micelles) (Romanini *et al.,* 1999). However, this process is responsible for spectroscopic changes. AmB molecules were organized in a form of tube like hydrophilic species. Chromophores were stacked parallely inside the aggregate and surrounded by hydrophilic parts of AmB molecules. Geometrical parameter of the model depends on a number of molecules forming the linear, cylindrical aggregation as shown

in Figure 1.2. The spectrum can be adequatedly reproduced for aggregates containing 4 to 8 AmB molecules. The distance between neighboring chromophores only slightly depends on the number of the molecules and varies from 1.33 to 1.4 nm. A radius of chromophores tube was more dependent on molecules. It varies from 0.94 nm in the tetramer to 1.83 nm in the octamer. Tube like micelles could also associate in the head to tail pattern (Gruszecski *et al.,* 2003). The next step, AmB in aqueous medium have a strong tendency to reduce the surface of apolar parts exposed to water. This is a straight way to reduce the interaction with other monomeric molecules. The larger dimers may subsequently interact to continue diminishing of hydrophobic by formation of hydrophilic, colloid type micelles until the larger dimers cannot detect in spectroscopic properties of the solution because the micelle structure is chaotically organized (Mazerski and Borowski, 1996).

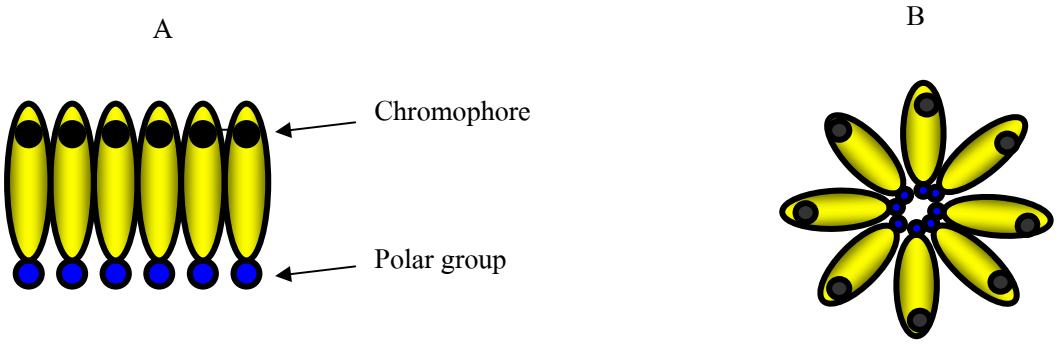

Figure 1.2 Aggregation structure of Linear aggregation (A), Cylinder aggregation (B) (adapted from Gruszecski *et al.,* 2003).

When AmB was dispersed in aqueous medium, UV absorption of AmB shows four well separate bands at 344, 365, 385 and 410 nm. It is characterized as monomeric state of AmB as

shown in Figure 1.3(A). When the AmB solution was left at the room temperature for 5 days, the spectrum of broad single band at 328 nm accompanied by decreasing in intensity at 365, 385 and 410 nm was characterized as aggregated state of AmB. AmB change to dimeric is shown in Figure 1.3(B) (Romanini *et al.,*1999 and Gruszecski *et al.,* 2003).

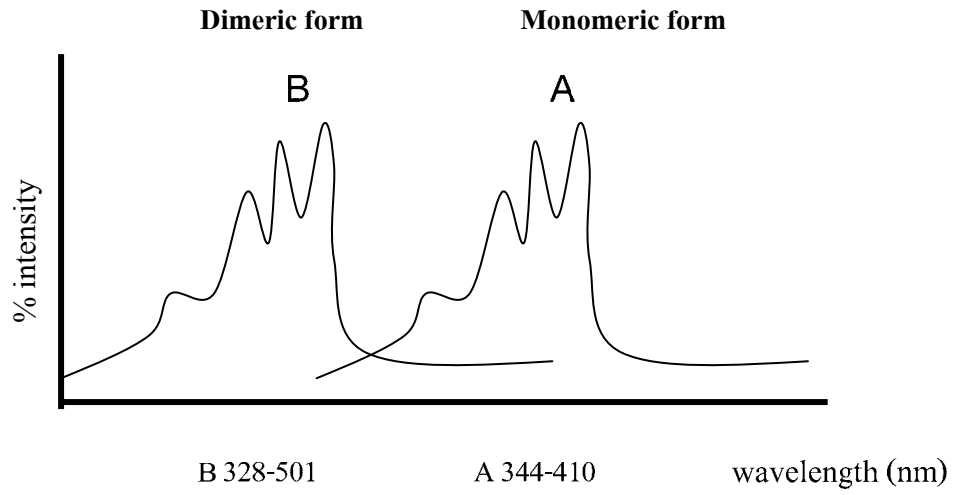

Figure 1.3 The UV band absorption of AmB in aqueous medium, the monomeric form (A), the dimeric form after 5 days (B)

The relative aggregation state of the AmB links with AmB toxicity (Romanini *et al.,*1999). The self aggregation of AmB leads to decreased water solubility resulting in poorly absorbed from the gastrointestinal tract. It can accumulate in tissue and organ and cause toxicities especially nephrotoxicity and hemolysis.

1.2.2 Nephrotoxicity

The incidence of conventional AmB nephrotoxicity is 49-65% (Chavanet, 1997). It is associated with vasoconstriction causing ischemic injury and direct interaction with epithelial cell membranes causing tubular dysfunction. This is a dose dependent and cause of prolonged hospitalization and increased mortality especially if the patient needs hemodialysis (Antoniadou and Dupont, 2005). Dimeric AmB is able to bind to the kidney epithelial cells, finally cause nephrotoxicity. There are two types of the AmB formulations; a micellar solution of AmB with deoxycholate as surfactant that causes serious nephrotoxicity and other is lipid based formulations. Unfortunately, lipid based formulation frequently needs the use of glutaraldehyde or formaldehyde that may cause nephrotoxicity (Tiyaboonchai and Limpeanchob, 2006). The new technique involved the self-assembly of polyelectrolytes and used of the oppositely charged aqueous soluble polymers (chitosan, dextran sulfate, MPEG). These advantages help AmB in polymer to give good solubility. However, the bonds are a labile carbamate that is easy to cleave in the blood and easily release free AmB (Sedlak *et al.,* 2007).

1.2.3 Hemolysis

The aggregated and monomeric forms of AmB seem to be crucial with respect to non selective toxicity especially hemolysis in erythrocyte (Legrand *et al.,* 1992). The mechanism of hemolysis has related to ion permeability and lipid peroxidation. AmB is large polyene macrolides, comprising non aromatic heptenes and are channel-forming antibiotics and it is due to

rather specific increase of permeability mainly to monovalent cations (primary effect). The flux of ions through the channel formed in the cell membrane leads to a hemolysis (secondary effect). In addition, a colloid osmotics and lipid oxidation that occur have been related with hemolysis (Cybulska *et al.,* 1995). Infact, the permeability to monovalent cations and ion flux is an essential step preceding hemolysis and lipid peroxidation seems to be a secondary event in the hemolysis process related to ion flux and swelling. However, erythrocytes are very sensitive to the toxic effects of polyene macrolides. Yu *et al*. (1998) demonstrated the ability of surfactant to reduce the toxicity of AmB via decreasing the aggregation state of the drug, a carrier capable of minimizing the aggregation state of AmB is desirable. Adams *et al*. (2003) observed time dependent hemolysis activity of the pure AmB, AmB in micelle, and buffer (Figure 1.4). It was found that AmB in micelle caused 40 % hemolysis while pure AmB produced 80 % lysis after 24 h. The AmB in micelle was less hemolytic than pure AmB due to the interaction of AmB with side chain of micelle. Therefore, free AmB might slowly dissociate from AmB micelle, which may reduce the hemolytic effect of AmB.

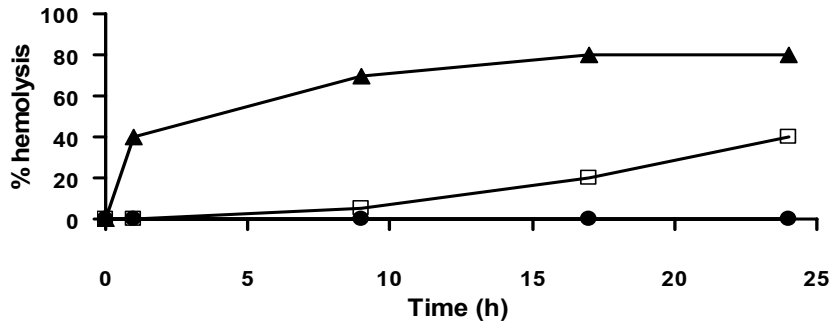

Figure 1.4 Time dependent hemolysis profile of AmB (▲) (~3 µg/ml), AmB-loading surfactant micelles formulations (□) and buffer (●) (Adams *et al.,* 2002)

The hemolysis of AmB is not only time dependent but also concentration dependent. The presence of a lag phase is related to AmB thresholds necessary for pore formation in the target cells. A carrier vehicle may delay the onset of pore formation by limiting the diffusion of free AmB into aqueous medium. Thus, the hemolysis may decrease through such a mechanism.

1.2.4 Cost of AmB

Cost is a big issue when using a lipid formulation AmB. Clinical studies have been proved that the cost of treatment with lipid formulation AmB can be overweighed by the cost of nephrotoxicity as shown in Table 1.1.

Table 1.1 Average cost therapy of AmB in various formulations for one week (Antoniadou and Dupont, 2005)

Total cost	**Conventional**	**Lipid formulation AmB**		
	AmB	**ABCD**	**ABLC**	**LAmB**
Typical daily dose (mg/kg)	1	4	5	5
Estimate weekly cost (US $)	260	3360	5800	9200

The mortality and cost of renal failure associated with AmB therapy were reported among 707 admissions treated with AmB, 30% developed acute renal failure with consequences

of prolonged hospitalization (8.2 days), higher mortality and increased cost per episode ($30,000) (Robinson and Nahata, 1999). Lipid formulations of AmB and conventional AmB were compared in terms of effectiveness and tolerability in patients with systemic fungal infections. It was noted that there was no difference in efficacy. Nephrotoxicity risk was reduced by 58% in patients treated with lipid formulation and importantly mortality was reduced by 28% in the same group (31 patients treated with lipid formulation AmB) (Antoniadou and Dupont, 2005).

1.3 Proposed research

In order to solve aforementioned problem of AmB, advanced drug delivery technology has been employed. Much effort has been spent to develop delivery system with reduced amphotericin B toxicity. The liquid crystals are considered to be used as drug delivery systems. As they have a potential in control release rates, thus reduce toxicity may be posible. It may also increase in the solubility of drugs by means of solubilization. The characteristic of liquid crystal is considered as the fourth state of material (i.e. solid, liquid, gas and liquid crystal). Liquid crystals flow like a liquid, but they are anisotropic compounds. From our preliminary data, we found that deoxycholic acid (DCA) linked to hydrocarbon chains by ether bond and has liquid crystal properties. It was named cholate cetyl ether (CCE), as shown in Figure 1.5.

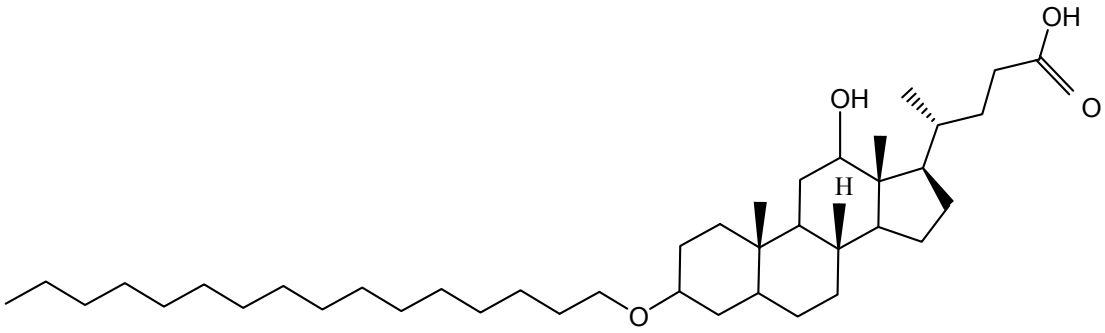

Figure 1.5 The structures of cholate cetyl ether (CCE)

The CCE structure is closely related to "bile acid with amine conjugates synthetic inophores" as shown in Figure 1.6 (Umgawa *et al*., 1984). The bile acid with amine showed moderate antifungal activity (Salunke *et al.,* 2003). It was found to be active (IC_{50}= 62.5 µg/ml) against *C. neoformans*. It was suggested that these compounds could transport the ion across the phospholipid bilayer.

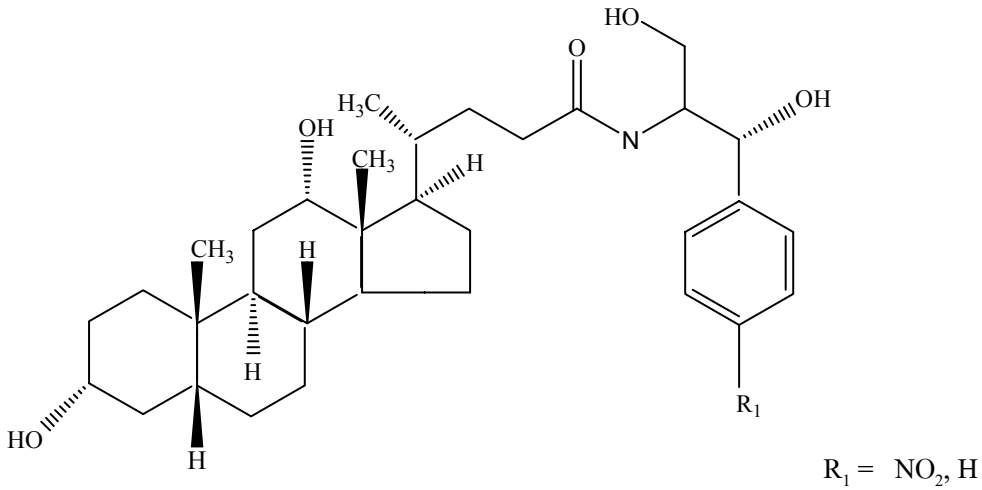

Figure 1.6 Design of ionophore of bile acid with amine (Salunke *et al.,* 2003)

The synthesis of such molecules has intensified in the development novel ionophoric devices. The ultimate goal of this study is expected to obtain synergistic effect of AmB in CCE that can punch holes in the membrane of fungal cells, but not in mammalian membranes. This might lead to expect that AmB in CCE can directly penetrate to fungus membrane. These strategies could minimize the adverse drug reaction. The model structure of AmB in CCE is shown in Figure 1.7. AmB may insert between CCE molecule by positioning the polar head group outward and hydrophobic part inward. These structure orientations may improve solubility of AmB. AmB-CCE may form a nanodelivery system.

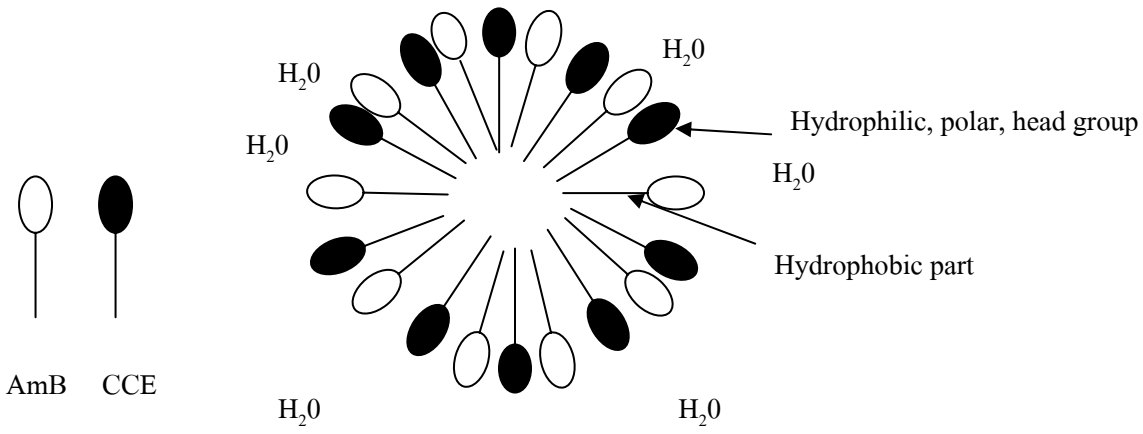

Figure 1.7 Model structure of AmB in CCE nanosystem

1.4 Objectives of thesis are as follows

1. To synthesize and purify CCE
2. To study chemical and physical characteristic of CCE
3. To evaluate stability of AmB in CCE
4. To evaluate susceptibility of AmB in CCE
5. To evaluate toxicity of AmB in CCE

CHAPTER 2

REVIEW OF LITERATURES

2.1 Fungal cell structure and targets

The cell membrane contains lipid particle called the sterol. The sterol in fungus is different from that of mammalian cell membrane. The ergosterol is the main sterol in fungal membranes, whereas cholesterol contains in mammalian cell. Several classes of antifungal agents including the polyene, azole and allylamines have exploited the difference in sterol content as the target action (Russell, 2007).

2.2 Molecular basis of sterol specificity of polyene

The polyene macrolide antibiotics remain most promising as a source of potential antifungal drugs of clinical significance. This group of compounds, unlike other antifungal drugs, combines all features essential for the effective antifungal drugs. The polyene contains of the large macrolide heptene ring. It exhibits a high specificity of membrane effects related to channel formation. AmB is only one member of this group of antibiotics that use in clinics for the treatment of systemic infections. AmB prefers to bind ergosterol better than cholesterol. The model shows that eight AmB molecules can insert in the bilayer with polar (OH groups) in the

center, arranging like barrel staves sandwiched alternately with sterol molecule (Coreto *et al*., 1998 and Matsumori *et al*., 2004) as shown in Figure 2.1.

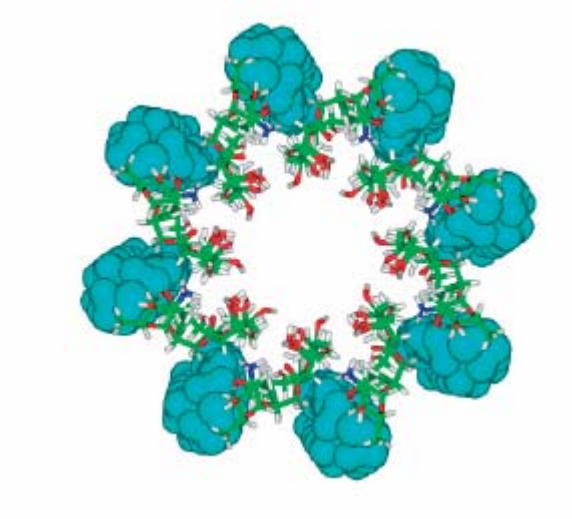

Figure 2.1 Model structure of AmB-ergosterol channel. The channel contains eight AmB molecules (stick-occurred by atom type) and eight ergosterol molecule (blue) (Matsumori *et al*., 2004).

The binding of AmB with fungal cell membrane involves in the hydrogen bonds between the hydroxyl groups of the sterol and the carboxyl group at C_{18} of the AmB molecule. The strong intermolecular AmB–sterol interactions within the channel are responsible for its stability (Cotero *et al*., 1998). This binding is strengthened by participation of the amino group of the amino sugar as shown in Figure 2.2.

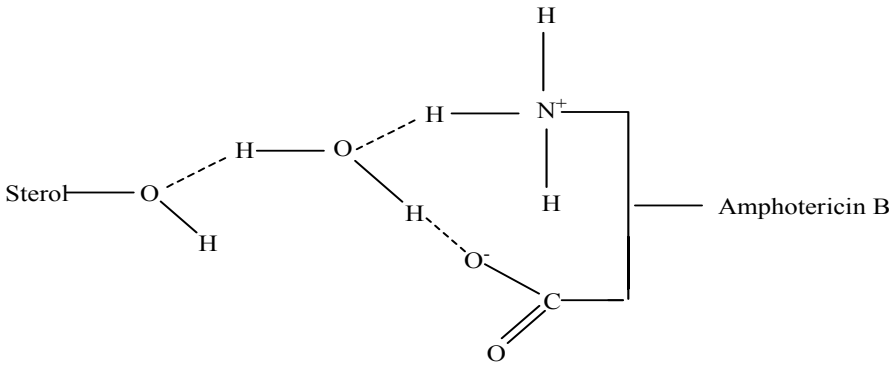

Figure 2.2 Schematic representation of hydrogen bond formation (Brajtburg *et al*.**,** 1990).

The mechanism why AmB channels are more effective in membranes containing ergosterol molecules, involving the rigid chain of seven conjugated double bonds of AmB and the whole sterol molecule by van der waals forces. Due to lower conformational freedom of ergosterol side chain may have better van der waals contacts with an AmB molecule than that with cholesterol. The flat shape of the ergosterol molecule may facilitate intermolecular contacts with the polyene macrolide (Brajtburg *et al*., 1990). Therefore, it appears that van der waals forces are decisive for the specificity of AmB for ergosterol, whose conformational state is most favorable for this kind of interaction while the cholesterol side chain without the double bond at C_{22} is more flexible. It revealed that ergosterol exhibits a very different electrostatic potential compared to the cholesterol molecule (Baginski *et al*, 1997). The thermodynamic studies of the AmB channel permeability showed that both cations and anions can enter and pass through the pore. No substantial barriers for either cations or anions were found. This finding may be explained by the fact that AmB channels are quite large compared to many protein channels.

It means that ions passing through the channel are not forced to strip out water molecules forming the solvation shell of each ion. On the other hand, differences between the diameters of AmB–ergosterol and AmB–cholesterol channels revealed that in the case of the AmB–cholesterol channels, small potential well trap for cations can be formed at the entrance to the channel. This observation may explain to some extent why AmB–cholesterol channels, even when formed are not good carriers of cations. The AmB bind sterols incorporated in cellular membrane results in disorganization of the membrane, possibly by formation of specific pores composed of small aggregates of AmB and sterol. These defects cause depolarization of the membrane and increase in membrane permeability to K^+, Na^+, and H^+ flux into cell membrane irregularly, causing the leakage of intracellular electrolyte with subsequent cell death (Brajtburg *et al*., 1990) as shown in Figure 2.3. The binding of AmB with sterol membrane occurs by endocytosis. LDL receptors are thought to play a role in this uptake, AmB bound to LDL is internalized with phagolysosomes by macrophage (Hartsel and Bolard, 1996). The mechanism occurs on transmembrane pore. In the mammalian cell, this reaction occurred above concentrations threshold of drug self-association whereas with the fungal cell, it may occur much below the thresholds as shown in the Figure 2.4.

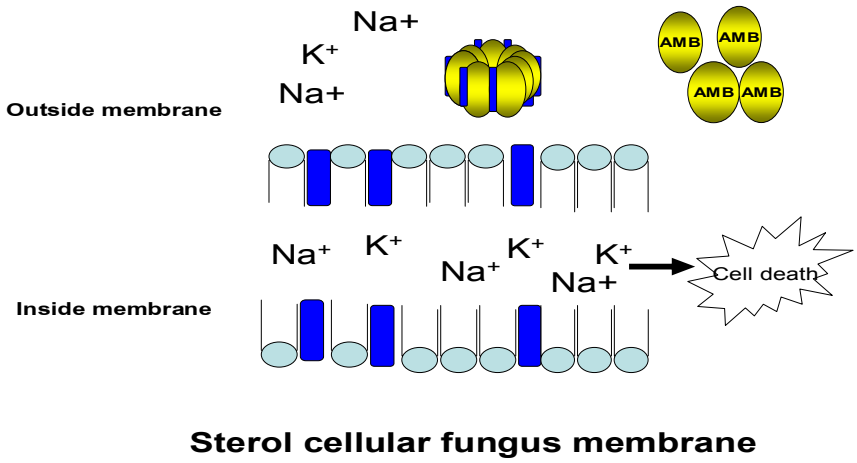

Figure 2.3 Mechanism of AmB on transmembrane pore in fungal cell

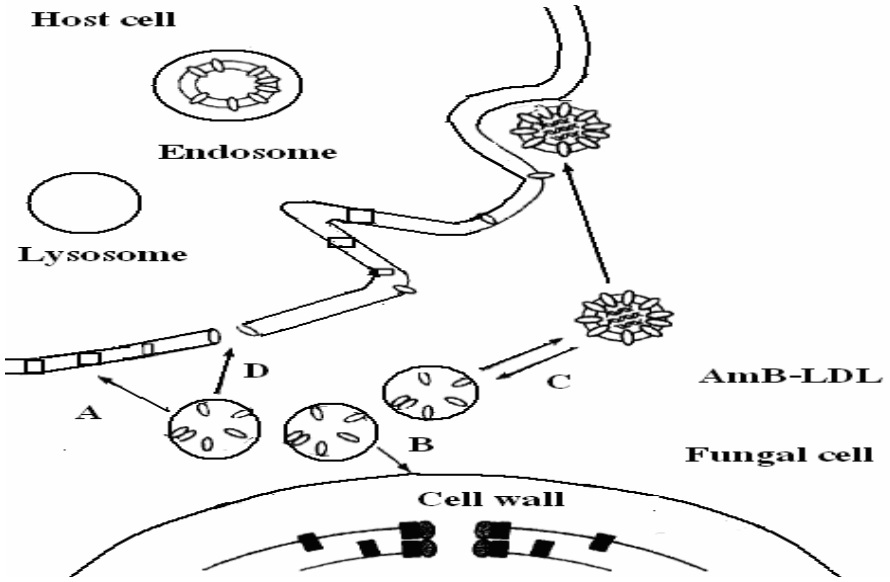

Figure 2.4 Formation mechanism of AmB-LDL receptor on the transmembrane pore with mammalian cells. This formation only occurs for AmB concentrations above threshold of drug self association (A), with fungal cells it may occur much below the threshold (B), AmB bound to LDL is internalized (C), lipid peroxidation makes membranes more fragile (D). Amphotericin B (○), cholesterol (□), ergosterol (■) (Hartsel and Bolard. 1996).

2.3 Effect of AmB with oxidation dependent events in stimulatory lethal effect

It was found that the active oxygen species of AmB is linked with lytic or lethal actions of fungal cell membrane. The mechanism of AmB-induced oxidative suggests two processes by which AmB affects cells. The first is auto-oxidation of AmB and the formation of free radicals. The free radicals formed in this process may have several different effects on cells among them is stimulation. Stimulation, as well as other effects, may thus originate from the auto-oxidation of AmB bound to membrane components. In this case, oxidative events do not link to membrane permeability and are not dependent on the kind of sterol. The second mode of action may result from AmB-induced increase of membrane permeability, especially to monovalent cation (Brajtburg *et al*., 1990).

2.4 AmB against *C. neoformans*

C. neoformans is an encapsulated yeast-like fungus that can live in both plants and animals (Dadachova, 2005). These species, also known by its teleomorph name, *Filobasidiella neoformans*, belongs to the broad class of organisms called "club fungi" or Division Basidiomycota, which is one the five major types of fungi. *C. neoformans* usually grows as yeast (unicellular) and replicates by budding. Under certain conditions, both in nature and in the laboratory, when grown as yeast, *C. neoformans* has a prominent capsule composed mostly of polysaccharides. Microscopically, the Indian ink stain is used for easy visualization of the capsule. The particles of ink pigment do not enter the capsule that surrounds the spherical yeast

cell, resulting in a zone of clearance or "halo" around the cells. Incident of infection due to *C. neoformans* has remained important in both non-HIV and HIV patients (Nooney *et al*., 2004). The MICs of amphotericin B by the broth microdilution methods as recommended by the National Committee for Clinical Laboratory Standards (NCCLS) was 0.04-2.8 μg/ml while MICs of 98 isolates of *C. neoformans* were obtained from the cerebro spinal fluid between HIV infected patients diagnosed cryptococcal meningitis to 2 groups including Group A and B. The median (range) MICs of AmB was 0.25 (0.03-1.0) μg/ml in group A and 0.25 (0.12-1.0) μg/ml in group B (p=0.384) (Weerawat, 2006). The criteria for susceptibility of AmB are ≤ 1 μg/ml and > 1 μg/ml for resistance (Therase *et al.,* 2006).

2.5 Research and development of AmB

There are two dosage forms of AmB available nowadays. The first dosage form is conventional dosage. The potentially deleterious detergent was used to solublize the drugs in micelles for intravenous administration. Later, liposome encapsulated AmB was developed to overcome the side effect from conventional AmB. It was lipid formulation of AmB (Bekersky *et al*., 1999). The research and development of AmB are summarized as follows.

2.5.1 Conventional AmB

Fungizone™ formulation is a colloidal suspension of AmB. Sodium deoxycholate was used as a solubilizing agent and micelle formation in this formulation. Fungicidal activities

depend on a concentration of drug in various body fluids and the susceptibility of the fungus. Clinical applications are also in non invasive forms of fungal infections such as oral thrush, vaginal candidiasis and esophageal candidiasis (Chavanet**,** 1997). AmB deoxycholate is available as a 50 mg vial of lyophilized powder for injections. It is reconstituted only with sterile water without preservatives (not bacteriostatic water containing benzyl alcohol, sodium chloride or other electrolyte solution due to AmB precipitation/aggregation). The solution may then be diluted with 5, 10 and 20 % dextrose injection for IV infusion. Final concentrations should not exceed 0.5 mg/ml in 5 and 10 % dextrose injection. After dilution, formulation can be administered through a central catheter via an in line filter. However, if peripheral administration is necessary, concentrations should not exceed 0.1 mg/ml in 5 % dextrose injection over 1-4 h (Caillet *et al*., 1995).

Despite broad-spectrum antifungal activity, the clinical use of AmB is limited by nephrotoxicity, which leads in some cases to permanent renal impairment, especially in the presence of other nephrotoxic drugs such as aminoglycosides, NSAIDs, furosemide and cisplatin. The endpoint of treatment is generally determined by the resolution of the neutropenia or improvement after discontinuation of corticosteroid rather than by the cumulative dose.

Several strategies have been used to minimize nephrotoxicity including saline loading, alternate-day dosing, and AmB dose reduction. To improve the tolerability profile and enhance efficacy, extensive efforts were made to reformulate AmB by replacing sodium deoxycholate with either phospholipids or cholesterol (Espuelas *et al*., 1997).

2.5.2 Lipid formulations of AmB

2.5.2.1 Liposomal AmB (LAmB) or Ambisome

Liposomal AmB contains unilamellar liposomes. The AmB is encapsulated inside the liposomes as shown in Figure 2.5 (Mehta *et al.*, 1984). This formulation employed saturated (rigid) phospholipids with cholesterol to stabilize the liposomal membrane. A charged phospholipid (phosphatidylglycerol) was also included to stabilize the AmB liposomes through ionic interactions (Fournier *et al*., 1998). Further stabilization could result from the direct interaction of AmB with cholesterol via its sterol binding region. It was anticipated that the small size of these liposomes (<100 nm) would provide stabilization in vivo and prolong the circulation of drug containing liposomes in the plasma. However, in order to maintain a true liposomal formulation, the content of AmB had to be about 10% by weight.

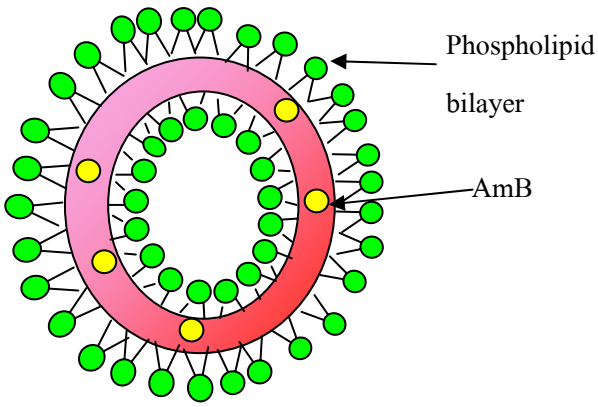

Figure 2.5 Liposome AmB structure

2.5.2.2 AmB lipid complex (ABLC)

A lipid complex consisting of AmB and the lipids dimyristoylphosphatidylcholine and dimyristoylphosphatidylglycerol in 1:1 molar ratio as shown in Figure 2.6, it can be called "ABLC". It possesses a ribbon like structure resulting in a higher molar ratio of AmB product. Due to its large size, ABLC is rapidly cleared from the circulation via the reticuloendothelial system. It is believed that phospholipases released by vascular smooth muscle as well as those derived from macrophages and released by infecting fungus would breakdown the lipid complexs to AmB, thus releasing the drug at the infected site which may reduce the nephrotoxicity (Mehta *et al*., 1984, Robinson and Nahata, 1999 and Bekersky *et al*., 1999)

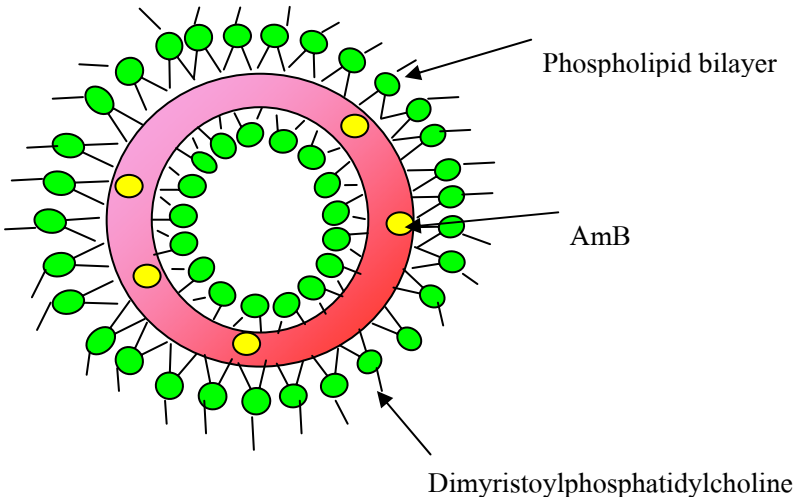

Figure 2.6 AmB lipid complex (ABLC) structure

2.5.2.3 AmB colloidal dispersion (ABCD)

AmB colloidal dispersion is the only lipid formulation that contains true liposomal form structures. ABCD is AmB complex with cholesteryl sulfate in about 1:1 molar ratio as shown in

Table 2.1. ABCD leads to reduced concentrations of plasma lipoprotein associated AmB, and thus lower concentrations of free AmB in the kidney. The rapid removal of the complex also prevents high peak serum concentrations of AmB after infusion of AmB. The improved safety profile of AmB colloidal dispersion over conventional AmB was confirmed in the studies, however, a third of patients experienced chills and fever after initial dosing (Wong-Beringer *et al*., 1998, Bekersky *et al*., 1999 and Robinson and Nahata, 1999).

Table 2.1 Composition and structure of lipid–based AmB formulations (Antoniadou and Dupont**,** 2005)

Formulation	Structure	Particle size (nm)	AmB:lipid ratio
ABLC (Abelcet®)	Ribbon-like complex	1600-11600 in length	Dimyristoyl phoshatidylcholine dimyristoyl phosphatidylglyceol (7:3)
L-AmB (Ambisome®)	Liposome	45-80 in diameter	Hydrogenated soy phoshatidylcholine: Cholesterol: distearoyl phosphatidylglyceol (10:5:4)
ABCD (Amphotec®)	Disk like shape	120-140 in diameter 4 *thickness	Cholesteryl sulfate

These lipid formulations differ in several aspects, in their lipid composition, shape, physicochemical properties as shown in Table 2.1. They exhibit differences in clinical efficacy and share different accumulation rates to various tissue components. AmB formulations are often highly lipophilic and insufficiently soluble in aqueous media (Antoniadou and Dupont**,** 2005). Although nephrotoxicity of lipid formulations is less than conventional AmB and lipid formulations are better tolerated allowing the administration of higher doses but cost and other factors limit their widespread use in clinic (Larabi *et al*., 2004).

2.6 Liquid crystal and research development

2.6.1 Definition

Liquid crystals are organic compounds that are in a state between liquid and solid forms. They are viscous**,** jellylike materials that resemble liquids in certain respects (viscosity) and crystals in other properties (light scattering and reflection). Typical liquid crystals have either a rodlike or a disclike shape, although many exceptions on this basic motif have been described (Friberg, 2000). Most liquid crystal are neutral organic compounds. In metallomesogens, a metal is incorporated in the molecule of the liquid-crystalline compound. Also minerals or inorganic compounds can form liquid crystalline phases (Binnemans, 2005). Driving forces for the formation of a liquid crystalline phase (mesophase) are interactions between the anisometric molecules (dipole-dipole interactions, van der Waal interactions, π-π stacking) (Saeva, 1979).

The liquid crystal are anisotropic materials and physical properties of the system vary with the average alignment with the director. If the alignment is large, the material is very anisotropic. Similarly, if the alignment is small, the material is almost isotropic. The phase behavior of liquid crystal materials are as follows:

- **Nematic phases**

The nematic liquid crystal phase is characterized by the molecule that has no positional order but tend to point in the same direction (along the director). Inside the molecules point vertically but are arranged with no particular phase. A special class of nematic liquid crystals is called chiral nematic. Chiral refers to the unique ability to selectively reflect one component of circularly polarized light. The term chiral nematic is used interchangeably with cholesteric (Binnemans, 2005).

- **Smectic phases**

The smectic state is another distinct mesophase of liquid crystal substances. Molecules in this phase show a degree of translational order not present in the nematic (Saeva, 1979). In the smectic phase, the molecules maintain not only the general orientational order of nematic, but also tend to align themselves in layers or planes. Motions are restricted within these planes and separate planes are observed to flow past each other. The increased order means that smectic state is more “solid like” than the nematic (Binnemans, 2005).

- **Cholesteric phases**

The cholesteric (or chiral nematic) liquid crystal phase is typically composed of nematic mesogenic molecules containing a chiral center which produces intermolecular forces that favor alignment between molecules at the slight angle to one another. This leads to the formations of a structure that can be visualized as a stack of very thin 2-D nematic like layers with the director in each layer twisted (Friberg, 2000).

- **Columnar phases**

Columnar Liquid crystals are different from the previous types because they are shaped likes disks instead of long rods. The stacked column of molecules characterizes this mesophase. The columns are packed together to form a two dimensional crystalline arrays. The arrangement of the molecules within the columns and the arrangement of the column themselves lead to new mesophase (Friberg, 2000).

2.6.2 Type of the liquid crystal

2.6.2.1 Thermotropic liquid crystal

The liquid crystal is formed by heating to a temperature above which the crystal lattice is no longer stable as shown in the Figure 2.7. The thermotropic liquid crystals are either smectic or nematic. The smectic phase is a layer structure, with parallel arrangement of the molecules along

their axis. In the nematic phase, the molecules are still aligned side by side, but not in specific layers (Saeva, 1979).

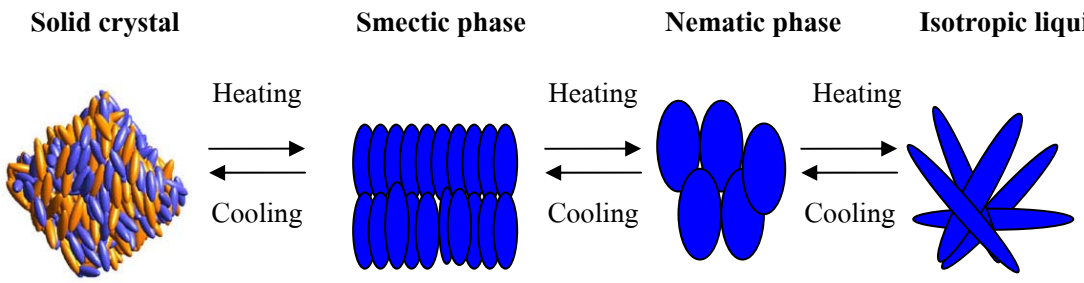

Figure 2.7 Arrangement of thermotropic liquid crystal

Figure 2.7 shows that thermotropic liquid crystals occur in a certain temperature range. If the temperature is raised too high, thermal motion will destroy the delicate cooperative ordering of the LC phase, pushing the material into a conventional isotropic liquid phase. At too low temperature, most LC materials will form a conventional (though anisotropic) crystal. Many thermotropic LCs exhibit a variety of phases as temperature is changed. For instance, a particular mesogen may exhibit various smectic and nematic (and finally isotropic) phases as temperature is increased. Smectic phases which are found at lower temperatures than the nematic, form well-defined layers that can slide over one another like soap. The smectics are thus positionally ordered along one direction.

2.6.2.2 The lyotropic liquid crystal

The lyotropic liquid crystals formed when certain compounds, amphiphilic molecules, are treated with a solvent. These compounds are characterized by a sort of split personality one end of the molecule is polar and attracted to water while the other end is nonpolar and attracted to hydrocarbons, or lipophilic (Friberg, 2000). A lyotropic liquid crystal consists of two or more components that exhibit liquid-crystalline properties in certain concentration ranges. In the lyotropic phases, solvent molecules fill the space around the compounds to provide fluidity to the system. In contrast to thermotropic liquid crystals, these lyotropics have another degree of freedom of concentration that enables them to induce a variety of different phases. A compound that has two immiscible hydrophilic and hydrophobic parts within the same molecule is called an amphiphilic molecule. Many amphiphilic molecules show lyotropic liquid-crystalline phase sequences depending on the volume balances between the hydrophilic part and hydrophobic part. These structures are formed through the micro-phase segregation of two incompatible components on a nanometer scale as shown in the Figure 2.8.

The content of water or other solvent molecules changes the self-assembled structures. At very low amphiphile concentration, the molecules will be dispersed randomly without any ordering. At slightly higher (but still low) concentration, amphiphilic molecules will spontaneously assemble into micelles or vesicles. This is done to 'hide' the hydrophobic tail of the amphiphile inside the micelle core, exposing a hydrophilic (water-soluble) surface to aqueous solution. These spherical objects do not order themselves in solution, however. At higher

concentration, the assemblies become order. A typical phase is a hexagonal columnar phase, where the amphiphiles form long cylinders (again with a hydrophilic surface) that arrange themselves into a roughly hexagonal lattice. This is called the middle soap phase. At still higher concentration, a lamellar phase (neat soap phase) may form, wherein extended sheets of amphiphiles are separated by thin layers of water (Nessem, 2001). For some systems, a cubic (also called viscous isotropic) phase may exist between the hexagonal and lamellar phases, wherein spheres are formed that create a dense cubic lattice. These spheres may also be connected to one another, forming a bicontinuous cubic phase. The objects created by amphiphiles are usually spherical (as in the case of micelles), but may also be disc-like (bicelles), rod-like, or biaxial (all three micelle axes are distinct). These anisotropic self-assembled nano structures can then order themselves in much the same way as liquid crystals do, forming large scale versions of all the thermotropic phases (such as a nematic phase of rod-shaped micelles). For some systems, at high concentration, inverse phases are observed. That is, one may generate an inverse hexagonal columnar phase (columns of water encapsulated by amphiphiles) or an inverse micellar phase (a bulk liquid crystal sample with spherical water cavities).

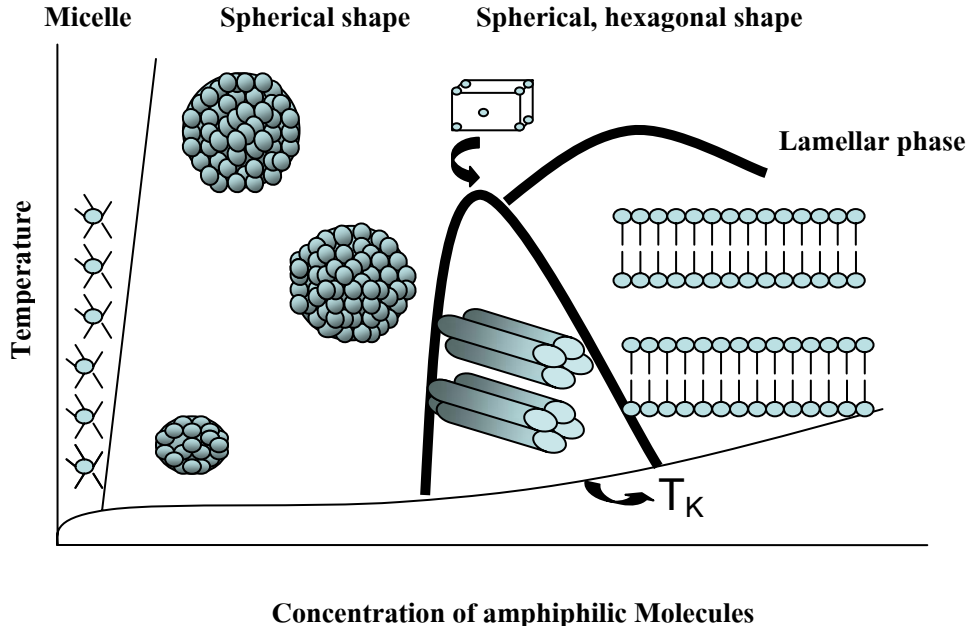

Figure 2.8 Changing of lyotropic liquid crystal formation above Kraft temperature (T_k)

2.7 Pharmaceutical research development in liquid crystal

Many studies have described the use of cholesteric liquid crystals in clinical thermometry (Lin *et al.*, 2000). This technique was used for temperature sensors to detect the defects and malfunctions in human beings by reflecting the skin temperature patterns from the liquid crystal thermogram. Cholesteryl oleyl carbonate (COC) (Figure 2.9) is one of the most popular cholesterol derivatives because it has a high temperature coefficient of the selective reflectance near room temperature (Lin *et al.,* 2001). Lin *et al* (1996) developed thermo-responsive membrane by entrapping COC into a cellulose nitrate membrane.

The COC embedded membranes was sensitive to minute temperature changes (Lin *et al.,* 1996). COC showed the thermotropic liquid crystal and lyotropic liquid crystal property. In addition, other derivative liquid crystals have the same properties such as cholesteryl benzoate, cholesteryl sulfate, cholesteryl pelargonate, cholesteryl nonanoate.

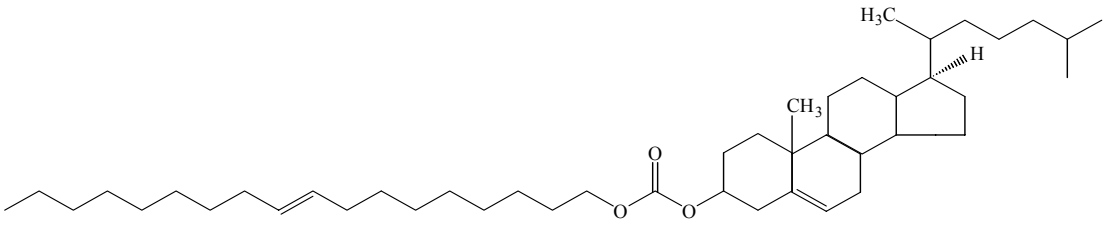

Figure 2.9 The structure of cholesteryl oleyl carbonate ester (COC)

Nowadays, liquid crystal incorporated in microcapsules made of gelatin which rupture on topical application are available in special dermatological formulations that exhibits hydrating properties. Most of all, liquid crystal are used as excipients to protect sensitive substances (vitamin, antioxidant, oils). They may enhance the stability of creams while creating a rheological barrier resulting in an increase in the viscosity and decrease in coalescence by modification of Van der Waals forces (Benita *et al*., 1996). One example is hydrocortisone. It is often taken in topical applications, but its use has been limited because the highest concentration can be only 1%. When the drug was blended into liquid crystal of lecithin and water, the concentration can be

up to 4 %. In time, liquid crystal may become a primary solvent for topical medications. Tolecine® and Apatone® are other drugs that use lyotropic liquid crystals in drug delivery. These lyotropic liquid crystals contain DNA, proteins and cholesterol. This drug was more effective to kill cancer cells than the current standard therapy. Therefore, liquid crystal is expected to have advantageous to deliver AmB that is highly toxic and prone to form aggregates in aqueous media. It is expected that COC and CCE as a carrier of AmB nanosystem can improve the efficacy and decrese toxicity of the AmB (http//www.kent.edu/media/NewsReleases/LCP.cfm).

CHAPTER 3

MATERIALS AND METHODS

3.1 Synthesis and characterization of CCE

3.1.1 Synthesis of CCE (Adapted from Wang and Huang, 2003)

CCE was synthesized from deoxycholic acid (Sigma-Aldrich, Steinheim Germany) and cetyl chloroformate at molar ratio 1:1 while cetyl chloroformate was obtained by reacting cetyl alcohol (Sigma-Aldrich, Steinheim, Germany) and triphosgene at molar ratio 3:1. The synthesis pathway of CCE is summarized in the Figure 3.1. Briefly, Cetyl alcohol 3 g (12 mM) was dissolved in 25 ml of dichloromethane (J.T. Baker, NJ, USA) in a clean and dry reaction flask kept in the ice bath until a clear solution was obtained and 1.0 ml of triethylamine (Sigma-Aldrich, Steinheim Germany) was added into the solution. Triphosgene 1.2 g (4 mM) was dissolved in 25 ml of dichloromethane and filled in burette, before adding dropwise into a reaction flask. The reation took 1 h and cetyl chloroformate was obtained. The cetyl chloroformate was further reacted with a deoxycholic acid 4.8 g (12 mM) in 25 ml dichloromethane released from the burette at one drop per 5 sec and 1 ml of triethylamine was added in the reaction flask again. The reaction was left overnight. The end product from the

reaction was purified by liquid-liquid extraction with water for three times. Organic phase containing liquid crystal mixture was collected and water residue was removed by adding 1 g of sodium sulfate (Fisher Scientific, Leicestershire, UK). The organic phase was dried using a rotary evaporator. CCE mixture was obtained as shown in Figure 3.1

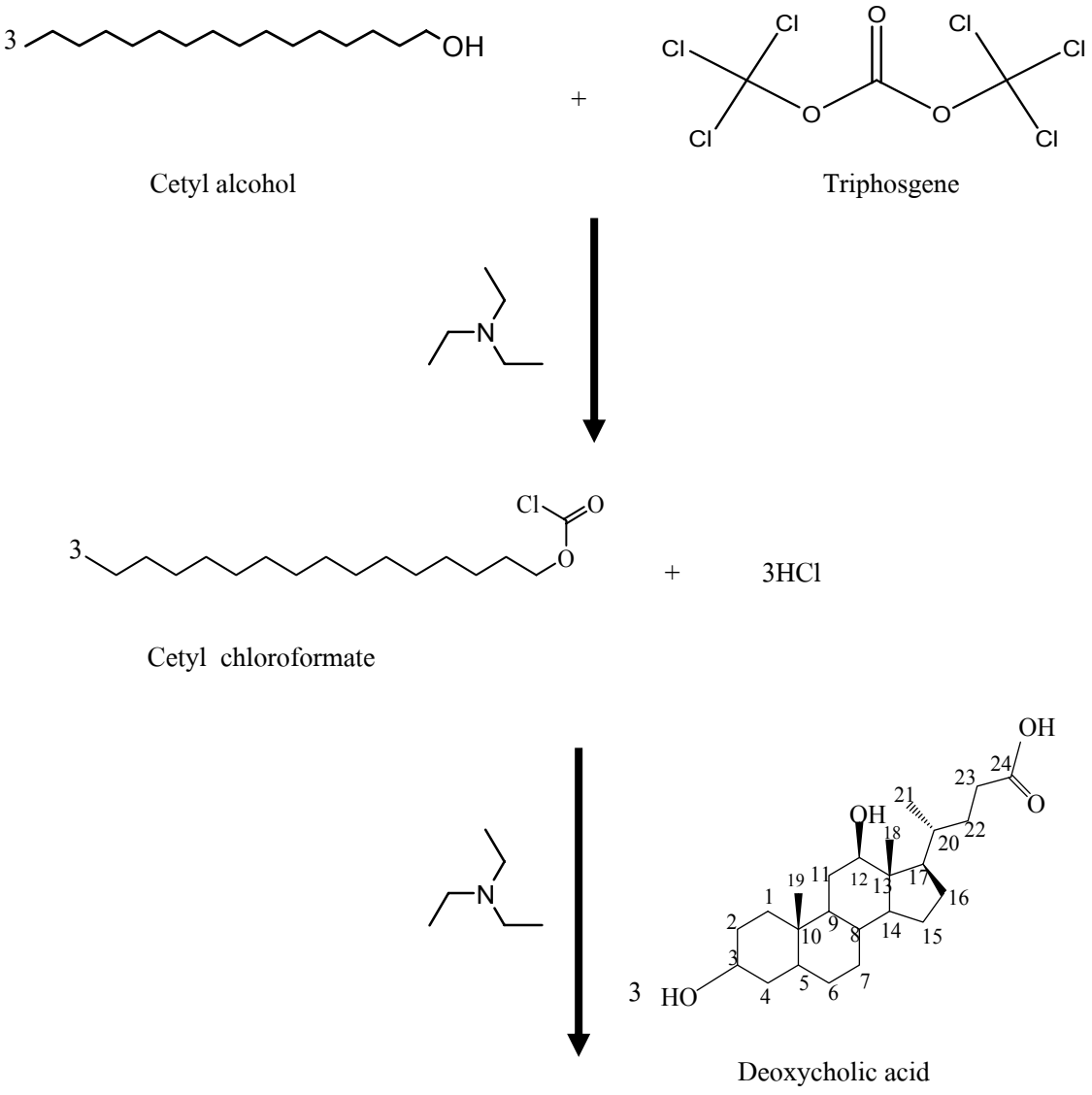

Deoxycholic acid

Figure 3.1 The synthesis and rearrangement of CCE structure

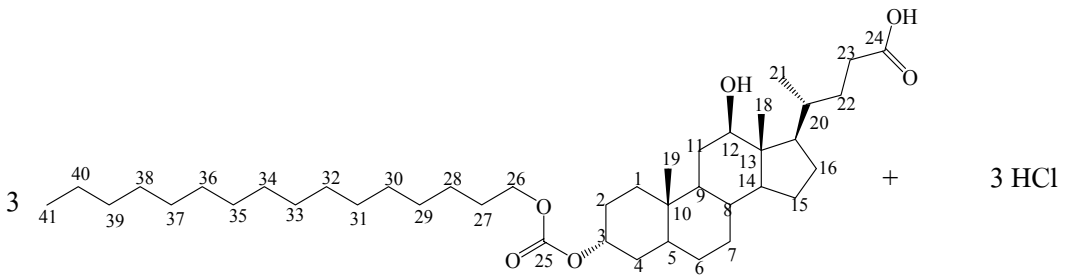

Cholate cetyl carbonate (CCC)

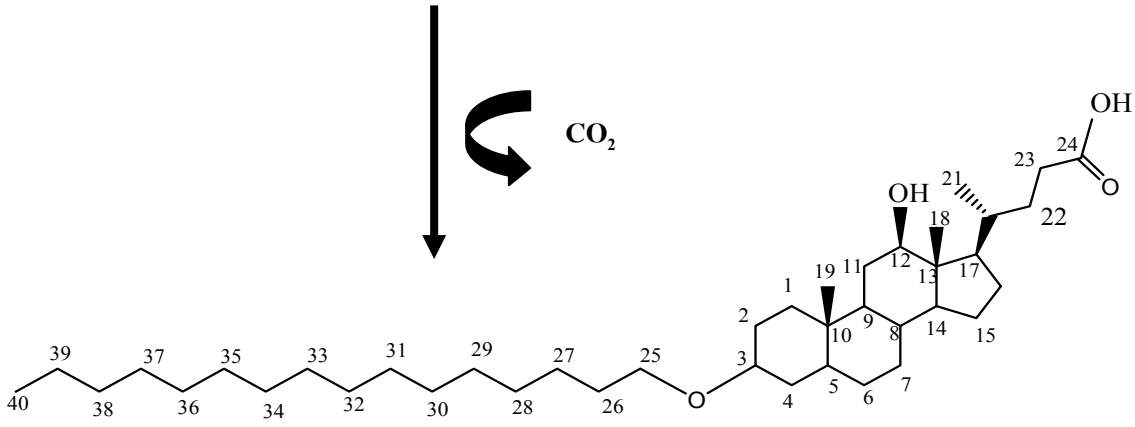

Cholate cetyl ether (CCE)

Figure 3.1 The synthesis and rearrangement of CCE structure (Continued)

- **Purification of CCE mixture**

CCE mixture that obtained from the reaction was developed on TLC system using 4:6 v/v hexane: ether (J.T. Baker, NJ, USA). The samples were detected by iodine vapor (Srichand united dispensary, Co.Ltd, Bangkok Thailand) and appeared as yellow-colored spots, Rf values were recorded. Flash column chromatography was employed to purify the liquid crystal by first 4:6 v/v hexane: ether with eluent flow rate of 2 ml/5 min for 30 min and followed by the second eluent, 50:50 v/v methanol: ethyl acetate, to elute the CCE mixture. The CCE in eluent was dried using a rotary evaporator. Finally, CCE was recrystallized in ethyl acetate: ether (4:1) by cooling down the solution in ice bath. Therefore, CCE was crystallized and separated the impurity from CCE crystal by decanting organic phase several times. CCE was collected and further dried by rotary evaporator.

3.1.2 Characterization of purified CCE

3.1.2.1 Fourier transform infrared spectroscopy (FTIR)

FTIR spectra were record by using a Spectrum GX series precisely (Model Equinox 55, Bruker., USA). FTIR spectra were recorded in the frequency range 4000-400 cm^{-1} and spectra were obtained at 4 cm^{-1} resolution under a dry air purge, accumulation of 32 scan and 2 zerofilling. A small amount of sample was sealed into KBr pellet by hydraulic press prior to measurement at ambient temperature.

3.1.2.2 NMR spectroscopy (^{13}C-NMR, ^{1}H-NMR)

CCE (30 mg) was dissolved in $CDCl_3$ in NMR tube, for ^{1}H-NMR and ^{13}C-NMR parameter was performed on Varian Unity at 500 spectrometer at 500 MHz (Varian, Germany). All the NMR spectra were recorded at 298 K using deuterochloroform ($CDCl_3$) as solvent. Chemical shifts were referenced to internal standard TMS.

3.1.2.3 Electrospray ionization mass spectrometry (ESI-MS)

ESI-MS (Bruker, Breman, Germany) with a positive mode was employed to identify the molecular mass of CCE. Direct injection technique was used in this study. The flow rate introduced into electrospay mass spectrometer (Perkin Elmer Sciex, API 300, CA, USA) was 39 l/h for cone gas flow and 343 l/h for desolvation gas flow. Operating voltage probe tip was 3200 V, sample cone was 50 V, extract cone was 5 V and RF lens was 275 V. The source temperature was 120 °C and the desolvation temperature was 130 °C. Molecular weights were scanned in range of 100-500 m/z.

3.1.2.4 Differential scanning calorimetry (DSC)

A differential scanning calorimetry (DSC) (model 2920, TA Instruments, New Castle, DE) was used to determine the thermal properties of CCE. The cooling rate was set at 5 °C/min from 50°C to -50 °C with a close pan system under the stream of N_2 gas. Transition temperatures

were determined as an onset of the transition peaks at which the tangential line of the inflection point of the rising part of the peak cross over the extrapolated baseline.

3.1.2.5 X-ray diffractometer (XRD)

X-ray diffractometer measurement were performed on a focusing camera in a 12 kW rotating anode X-ray generator (X'Pert MPD diffractometer, Philips, Wageningen, Netherland) with Cu K_α(λ = 1.54 °A) radiation at 40 kV and 60 mA. A double focusing Frank' s mirror was used to provide a highly focus beam. Sample was sealed in 1 mm-thick flat Kapton windows, placed in a sample holder. X-ray are collimated and directed onto the sample. As the sample and detector are rotated, the intensity of the reflected X-ray was recorded from 2θ of 2-60. When the geometry of the incident X-rays impinging the sample satisfies the Bragg Equation ($n\lambda = 2d \sin\theta$), constructive interference occurs and a peak in intensity occurs. The program PC-APD records and process X-ray signal and converts the signal to count rate.

3.2 Stability testing of AmB in liquid crystal

Stability testing of AmB in liquid crystal was monitored by UV spectroscopy and photon correlation spectroscopy (PCS). UV spectroscopy would not only indicate AmB stability, but also reveal whether the monomeric or dimeric form is present. While PCS helps to monitor size stability of AmB nanosystem. We also employed HPLC to monitor free and encapsulated AmB in AmB-liquid crystal nanosystem.

3.2.1 HPLC of AmB in liquid crystal

3.2.1.1 Preparation of standard solutions and AmB in liquid crystal

The 20 mg standard AmB (Ambalal Sarabhai Enterprise Ltd, Vodora, India) was weighed in volumetric flask and adjusted with DMSO to 10 ml. Each liquid crystal (DCA, COC or CCE) was weighed separately for 7.4 mg, dissolved with DMSO and adjusted to 10 ml. Standard AmB and liquid crystal in DMSO were used as a stock solution. AmB stock solution (5 ml) was pipetted into volumetric flask and adjusted to 10 ml with distilled water to obtain 1000 µg/ml of AmB. Finally, mixtures of AmB and each liquid crystal (DCA, COC or CCE) were prepared at a molar ratio 1:1 to obtain AmB at a concentration of 100, 10, 1 µg/ml whereas the liquid concentrations in the mixture were 74, 7.4 and 0.74 µg/ml in respective order. Pure AmB and each pure liquid crystal with similar concentrations as those contained in the mixture were prepared separately and used as a control samples. All procedures were done by pipetting 1000, 100 and 10 µl from each stock solution and made the volume to 10 ml with distilled water.

3.2.1.2 Chromatographic system and conditions

The HPLC system (Thermoelectron Corporation, CA, USA) used consisted of pump spectra system (T 2000) dual Auto sampler spectra system (AS 3000), Empower station (SCM 1000) and UV-VIS detector was used with a detection wavelength of of 383 nm. Separation was achieved using a isocratic elution accomplished on a Phenomenax® RP18, 10 µm (250* 4.6 mm,

i.d.) equipped with a guard column packed with Luna® C18, 10 µm. The mobile phase contained acetonitrite (J.T. Baker, NJ, USA) and water with a volume ratio of 40:60 v/v. The flow rate was 1.0 ml/min with an injection volume of 50 µl. The chromatographic system was validated in its linearity of the standard curve. Limit of quantification was calculated from six injections of each concentration of the standard curve.

3.2.2 Content of AmB in liquid crystal

The polyallomer thick wall tube containing 13 ml of samples was loaded into 45Ti swinging-bucket rotor with and axis of rotation about 110 nm. The samples were mixtures of AmB with either DCA, COC or CCE at a concentration of AmB 1 µg/ml. If the bubbles occurred during filling samples, they must be removed by tilting and rotating the tube before it was completely filled. The sample was centrifuged at maximum speed (41000 rpm) equal to relative centrifugal force of 288000 g for 7 h (Optima L-100 XP instrument (Bechman Coulter, C.A, USA). After ultracentrifugation, the sample was separated into two parts; yellow pellet of AmB at the bottom of the tube and the clear supernatant. The supernatant was used to analyze AmB by HPLC.

3.2.3 Chemical stability of pure AmB and AmB in liquid crystal

Chemical stability (molecular dynamic) of aqueous AmB (100 µg/ml) and AmB in liquid crystals (CCE and COC) from section 3.2.1 were recorded by UV spectrometer (Thermoelectron,

WI, USA). The UV–vis spectra were obtained using an absorbance range from 190 to 500 nm. Distilled water (Millipore, Watford, UK) was used as a blank. The UV spectrum was used as a tool to monitor AmB monomeric or dimeric form.

3.2.4 Size stability of pure AmB and AmB in liquid crystal

The particle size of AmB in liquid crystal (DCA, COC and CCE) at a concentration of 10 µg/ml from section 3.2.1.1 was determined by PCS (Malvern Zetasizer 4700, Worcestershire, UK) everyday for 15 days. The measurement was carried out at an angle of 90° while the temperature was maintained at 25 °C. All results of size stability were compared with that of pure aqueous AmB (10 µg/ml).

3.3 Microbial assay of pure AmB and AmB in liquid crystal

Cylinder plate method and Broth microdilution were used for microbial assay of AmB and AmB in liquid crystal. Cylinder plate data gives the relative potency of AmB in liquid crystal by determining the clear zone of AmB in liquid crystal in inoculum medium as compared with clear zone of AmB standard. Broth microdilution data can be used to calculate the minimum inhibitory concentrations (MIC). The MIC is based upon a predetermined endpoint, which may be interpreted as an absence of visible growth in broth containing known concentrations of AmB.

3.3.1 Potency of pure AmB and AmB in liquid crystal

3.3.1.1 Preparation of inoculum and inoculated medium

Potency of AmB and AmB in liquid crystal was screened by the cylinder plate method with *S. cerevisiae* (ATCC 9763, Rockville, MD, USA) approximately 10^8 CFU/ml. The *S. cerevisiae* was grown at 29-31 °C on the slant of antibiotic medium 19 (Difco, NJ, USA) for 48 h. The *S. cerevisiae* inoculum was prepared by adjusting to 25 % transmittance at 580 nm of bacterial suspension. Autoclaved antibiotic medium 19 was used as an inoculated medium. The inoculum (1ml) was mixed with 8 ml of autoclaved medium at 50 °C following by pouring into sterile plate. The plate was tilted back and forth to spread the inoculum evenly over the surface. The medium was left to cool down then put the plate in refrigerator at 4 °C for 1 h and dried at 37 °C for 10 min to remove surface moisture. The six assay cylinders with a radius of 2.8 cm and 12 mm in height were put slightly on the surface of each a plate by using a mechanical guide (adapted from Mcginnis and Rinaldi, 1991).

3.3.1.2 Preparation of standard solution and sample solution

AmB standard 10 mg was weighed and adjusted with DMSO to 10 ml and used as AmB stock solution. The AmB stock solution (1000 μg/ml) was pipetted for 0.64, 0.8, 1.0, 1.25, 1.56 ml into volumetric flask and adjusted with DMSO to 50 ml. Then AmB concentrations were 12.8, 16, 20, 25, 31.2 μg/ml. From each concentration, AmB solution 5 ml was pipetted and

adjusted by buffer No.10 to 100 ml. The final concentrations of standard AmB (S_1-S_5) were 0.64, 0.8, 1.0, 1.25, 1.56 µg/ml, respectively. The AmB sample solution was prepared by dissolving AmB 10 mg in DMSO 10 ml in volumetric flask thus the concentration was 1000 µg/ml. The 1 µg/ml of AmB in in liquid crystal were prepared by pipetting one hundred microlitres from both of 1000 µg/ml of AmB standard and 740 µg/ml of liquid crystal (DCA, CCE and COC) solution in volumetric flask. The AmB in liquid crystals were adjusted by buffer No.10 to 10 ml thus, the concentration of AmB in liquid crystals obtained was 20 µg/ml. Finally, five ml of this concentration was pipetted and adjusted with buffer No.10 to 100 ml in volumetric flask. The final stock solution of AmB in liquid crystals was 1 µg/ml.

3.3.1.3 Preparation of buffer NO10 (0.2 M, pH 10.5)

Dibasic potassium phosphate 35 g (Fluka, Switzerland) was dissolved in 1000 ml of distilled water and 2 ml of 10 N KOH was added into buffer No.10 (Analar, England) then adjusted pH of buffer No.10 by either 18 N phosphoric acid or 10 N KOH to obtain pH = 10.5.

3.3.1.4 Cylinder plate analysis

For the 1-level assay with a standard curve, prepare dilutions representing five test levels of the standard (S_1-S_5) and single test level of the Unknown U_3 corresponding to S_3 of the standard

curve, as defined under preparation of the standard and preparation of the sample. For deriving the standard curve, fill alternate cylinders on each of three plates with the mean test dilution (S_3) of the standard and each of the remaining nine cylinders with one of the other four dilutions of the standard. For AmB in liquid crystal (DCA, CCE, and COC) 1 µg/ml, fill alternate cylinders on each of three plates with the median test dilution of the standard S_3 and the remaining nine cylinders with corresponding test unknown solution (U_1, U_2, U_3) for AmB in DCA, COC, CCE. Repeat the process for the three dilutions of the standard and unknown solution. All plates were incubated at 29-31°C for 16-18 h, These experiment were carried out six times and the zone of inhibition was measured and calculated the concentration of AmB from standard curve and calculated cylinder plate method by measuring zone diameters (adapted from US Pharmacoepia 24 NF 19).

3.3.2 Susceptibility test with *C. neoformans* by broth microdilution

3.3.2.1 Preparation of inoculum

C. neoformans (Department of Pathology, Faculty of Medicine, Songklanakarin Hospital, PSU, Thailand) was subcultured on sabouraud dextrose agar (SDA) (Difco, NJ, USA) at 35 °C for 48 h. It should be subcultured 2 times, transferred some of cell growing with 85 % sterile normal saline then adjusted the inoculum suspension to 95 % transmittance at 530 nm, which was approximately 10^5 CFU/ml.

3.3.2.2 Preparation of sample stock solution

The concentration of AmB standard and liquid crystal was 2000 µg/ml The standard AmB allowed to sit at room temperature for 30 min then placed in container at 4 °C protected from light. The prepared AmB stock solution may be stored in the refrigerator for approximately 1 week.

3.3.2.3 Broth microdilution analysis

AmB in liquid crystal at 1:1 molar ratio were prepared by pipetting 16 µl from 2000 µg/ml of AmB stock solution and 12 µl from 2000 µg/ml of liquid crystal in volumetric flask, adjusted with antibiotic medium 3 broth (Difco, NJ, USA) to 10 ml. The concentration of AmB was 32 µg/ml. MICs were determined in a microtitre assay by inoculation of 5 µl of inoculum in 96-well plate with two-fold serials adding 100 µl of AmB in liquid crystal at concentration 32 µg/ml or AmB 32 µg/ml. The final concentration of sample test were 16, 8, 4, 2, 1, 0.5, 0.25, 0.125, 0.0625, 0.031 µg/ml. The well-plate No.11 was a positive control (growth promotion of inoculum) while well-plate No.12 was a negative control (sterility of medium). The plate was icubated at 35°C for 48 h and UV absorption was recorded at wavelength of 570 nm

3.4 Cytotoxicity evaluation of pure AmB and AmB in liquid crystal

Cytotoxicity evaluations were evaluated under two main studies; red blood cell hemolysis and cytotoxicity to alveolar macrophage and monocyte cell lines. The information from this study was served as a primary data whether AmB in liquid crystal is toxic or non-toxic

3.4.1 Hemolysis of pure AmB and AmB in liquid crystal

3.4.1.1 Hemolysis analysis

Human red blood cell (Blood Bank, Department of Pathology, Faculty of Medicine, Songklanakarin Hospital, PSU, Thailand) were isolated from fresh human blood, and the remainder was washed three times with phosphate buffer saline solution (PBS). The hemolysis was determined in the tube by pipetting 100, 50 , 10 µl from both of 1000 µg/ml of AmB standard and 740 µg/ml of liquid crystal from stock solution in section 3.2.1 with 0.2 ml of red blood cell and adjusted by PBS to be 10 ml. The concentration of AmB in liquid crystal that tested hemolysis was 10, 5, 1 µg/ml. The solution were incubated at 37°C in water bath and sampling at 0, 3, 6, 9, 12, 24 h and the unlysed cells in appendroff were removed by centrifugation at 1500 rpm for 10 min and hemoglobin in supernatant was determined by its absorbance at 550 nm. The positive control with 1% triton X-100 (Sigma-Aldrich, Steinheim, Germany) represents 100 % lysis and negative control sample with PBS without AmB represents 0 % and % hemolysis was

calculated using as Equation 1. The photos of lysed RBC and complete RBC were taken from light microscope at a magnification of 200 times.

$$\% \text{ Haemolysis} = 100 \times (Abs - Abs_0) / (Abs_{100} - Abs_0) \quad \textbf{Equation 1}$$

Where : Abs is the absorbance of sample

: Abs_0 is the absorbance of negative control

: Abs_{100} is the absorbance of positive control

3.4.1.2 Preparation of phosphate buffer saline (PBS) pH 7.4

KCl 0.2 g (Carlo Erba, Italy), NaCl 8 g (Merck, Damstadt, Germany), KH_2PO_4 0.2 g (Fluka, Buchs, Switzerland) and $Na_2HPO_4 12H_20$ 2.31 g (Fluka, Buchs, Switzerland) were dissolved in distilled water adjust to 1000 ml. add 2 ml of 10 N KOH (adjusted pH = 7.4 ±1 by 18 N of phosphoric acid or 10 N KOH).

3.4.2 Cytotoxicity of pure AmB, pure liquid crystal and AmB in liquid crystal with monocyte and alveolar macrophage

3.4.2.1 Preparation of Cell line

Rat alveolar macrophage cell line NR 8383 (ATCC Rockville, MD, USA) were cultured in modified Kaighn's modification Ham F12 medium (Gibco, Grand Island, NY, USA) with 2

mM L-glutamine adjusted to contain 1.5 g/l sodium bicarbonate (Gibco, Grand Island, NY, USA) supplemented with 15% (v/v) heat inactivated fetal bovine serum (FBS, Gibco, Grand Island, NY, USA), 50 units/ml penicillin and 50 μg/ml of streptomycin (Gibco, Grand Island, NY, USA). Mouse monocyte cell line J774.2 (ATCC Rockville, MD, USA) cultured in Dulbecco' s modified eagle medium (DMEM, Gibco, Grand Island, NY, USA) with 10% FBS and 50 units/ml penicillin, 50 μg/ml of streptomycin . All cell culture was incubated at 37 °C in 5% CO_2 incubator and 95% humidity incubator. The cell density of $5x10^5$ cells/ ml (100 μl) was seeded into each well and incubated overnight.

3.4.2.2 Preparation of sample

Two concentrations of AmB (200, 20 μg/ml) were prepared from the stock solution of 2000 μg/ml in DMSO by diluting with culture media: DMSO (9:1 v/v). Five concentrations of liquid crystal (DCA, COC, and CCE) at 360, 280, 200, 120, 40 μg/ml were prepared from stock solution diluted with the same solvent as that used in AmB. Ten concentrations of AmB in liquid crystals (DCA, COC, and CCE) were prepared in appendorf to obtain final concentrations of drug and liquid crystal at similar concentrations of pure sample.

3.4.2.3 Cytotoxicity determination of pure AmB, liquid crystal and AmB in liquid crystal

The cell line that counted by hemacytometer at 1* 10^5 cells/ml, 100 µl was cultured in each well plate and allow adhering and growth overnight under 37 °C in 5% CO_2 incubator and 95% humidity incubator. The day after, the fresh media (100 µl) was replaced and 100 µl of cell culture media containg either the pure sample, mixture in appendorf (100 µl) was loaded into each of 96 well plate containing cells after discarding the medium that was incubated overnight. Thus, the final concentration of the sample in the well was half of the sample concentration. Cultured media with diluted DMSO was used as a negative control. After incubation the AmB sample with cell line for 48 h, viabilities of sample were determined by using MTT (3-(4,5-dimethylthiazole-2-yl)-2 diphenyltetrazolium bromide (Sigma Chemicals ,St. Louis, MO, USA) to detect functioning mitochondria. The incubation was for 4 h at 37 °C. After that the supernatant was removed. The remaining formazan salt crystal was dissolved by adding 200 µl DMSO and determines the absorbance of formazan salt solution by microplate reader (Biohit BP 800, Helsinki, Finland) at a wavelength of 540 nm. The % viable cell was calculated according to the following equation compare to negative control (Equation 2)

$$\%\,viability = \frac{Abs\,sample}{Abs\,control} * 100 \qquad \textbf{Equation 2}$$

Where Ab_s is the absorbance of sample, Abs_o is the absorbance of negative control.

CHAPTER 4

RESULTS AND DISCUSSION

4.1 Synthesis and characterization of CCE

4.1.1 Synthesis of CCE

Cholate cetyl ether (CCE) was synthesized from coupling deoxycholic acid with cholesteryl chloroformate as shown in Figure 4.1. The chloroformate group is highly reactive with OH especially at position C_3. Whereas hydroxyl group at position 12 of deoxycholic acid did not react with acid chloride (Zhu and Nichifor, 2001). When the reaction is completed, the CCE mixture was obtained as off-white, odorless, sticky substance. The % yield of CCE mixture was about 70. The crude product was subjected to silica gel 60 TLC, using 40:60 v/v hexane: ether as a solvent system. The sample was detected by iodine vapor and appeared as yellow-coloured spots. From TLC (Figure 4.2), lane 1 shows a spot of deoxycholic acid which appeared at Rf 0.1, lane 2 reveals a spot of cetyl chloroformate with Rf 0.8. Moreover, Two spots of new compounds were found at lane 3 (Rf 0.3 and 0.7). The reaction mixture was purified by flash column chromatrography and was dried by rotary evaporator. The compound obtained at Rf 0.7 was a pink, odorless and appeared as semisolid at room temperature. However, from FTIR and NMR results (data not show), it was not a steroid compound whereas, the second compound at Rf 0.3

was examined by FTIR, NMR. It was promising results to be an expected product, therefore it was further tested by MS, XRD and DSC. Pure compound (Rf 0.3) shows an off–white, odorless and sticky substance at room temperature.

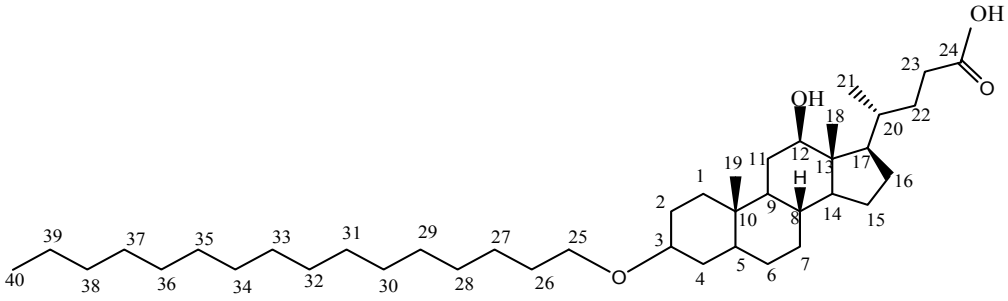

Figure 4.1 The structure of cholate cetyl ether (CCE)

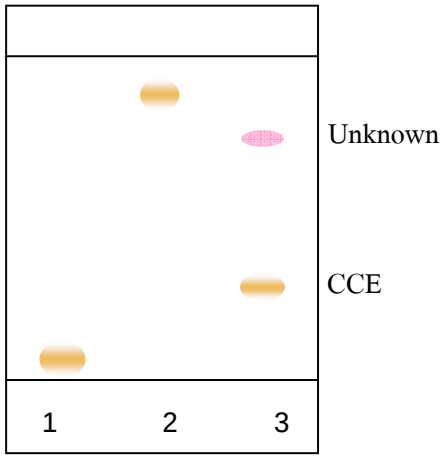

Figure 4.2 TLC of CCE mixture and starting materials: deoxycholic acid lane 1, cetyl chloroformate lane 2 and CCE mixture lane 3.

4.1.2 Characterization of purified CCE

4.1.2.1 FTIR spectrum analysis

Figure 4.3, The IR spectrum reveals 3 main peaks of methylene, ether and carboxylic group. The methylene group showed 2 distinct bands of C-H stretching that located at 2925 and 2872 cm^{-1}. These bands are relevant to the typical C-H stretching of methylene which located at 2856-2925 cm^{-1} (Silverstein, 1981). The band at 2925 cm^{-1} is the asymmetrical stretching mode while the peak at 2872 cm^{-1} is the symmetrical stretching mode. An ether group of CCE appeared at 1253-1039 cm^{-1}that is associated with the stretching vibration of the C-O-C systems. These vibrations involved with oxygen atoms result in greater dipole moment changes than those involving carbon atoms. The absorption bands of alkyl ether displayed an asymmetrical C-O-C stretching at 1275-1200 cm^{-1} and a symmetrical C-O-C stretching at 1075-1020 (Silverstein, 1981). The OH stretching of carboxylic group shows at wavenumber 3394 cm^{-1}. The band is very broad and high intensity in addition, carbonyl (C=O) stretching reveals at 1734 cm^{-1}. One of the characteristic bands in the carboxylic group was resulted from the out of plane bending O-H bond. This peak appeared at 946 cm^{-1} that gave broad band and medium intensity. Moreover, two bands arising from C-O stretching and O-H bending appeared at 1253 and 1461 cm^{-1}. Both of these bands were from the interaction between C-O stretching and in plane of C-O-H bending.

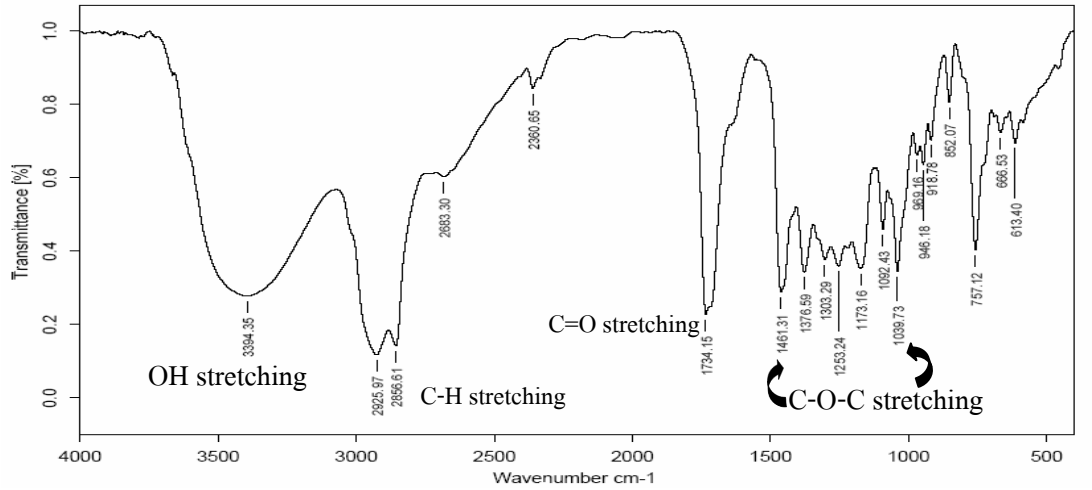

Figure 4.3 FTIR spectrum of CCE (KBr)

4.1.2.2 NMR spectrum analysis

The ^{13}C NMR spectrum of CCE gave 40 carbon atoms (Figure 4.4 A). ^{1}H NMR was employed to confirm the structure of CCE that found 69 protons as shown in Figure 4.4 B. The CCE spectrum was assigned by comparison of chemical shifts with deoxycholic acid and cholesteryl oleyl ether. ^{13}C NMR spectrum of CCE shows the chemical shift of a carbonyl carboxylate peak at 174.3 ppm and a presence of a new peak of alkyl carbon adjacent to the ether oxygen at 64.4 ppm. Other carbons in steroid part were located at chemical shifts (C_1-C_{19}) between 30.8-71.6 ppm. Table 4.1 gives assignments and chemical shifts for all carbons of CCE compared with deoxycholic acid (Vincent *et al.,* 1985). In addition, ^{1}H NMR spectrum of steroid part in CCE gave chemical shifts at 0.9-1.7 ppm. Excluding, methine proton at C_3 position appeared at 3.5 ppm, due to the unshielding of electron and high electronegativity of alkoxy group. Whereas, proton on methylene groups from alkyl chain gave similarly chemical shift at ~1.21 ppm and gave the highest intensity peak. However, protons on methyl groups were

resonanced at 0.67-0.92 ppm. Especially, proton on C_{40} showed the lowest chemical shift. The upfield shift at terminal carbon was attributed to the steric compression of a guache interaction (Silverstein, 1981).

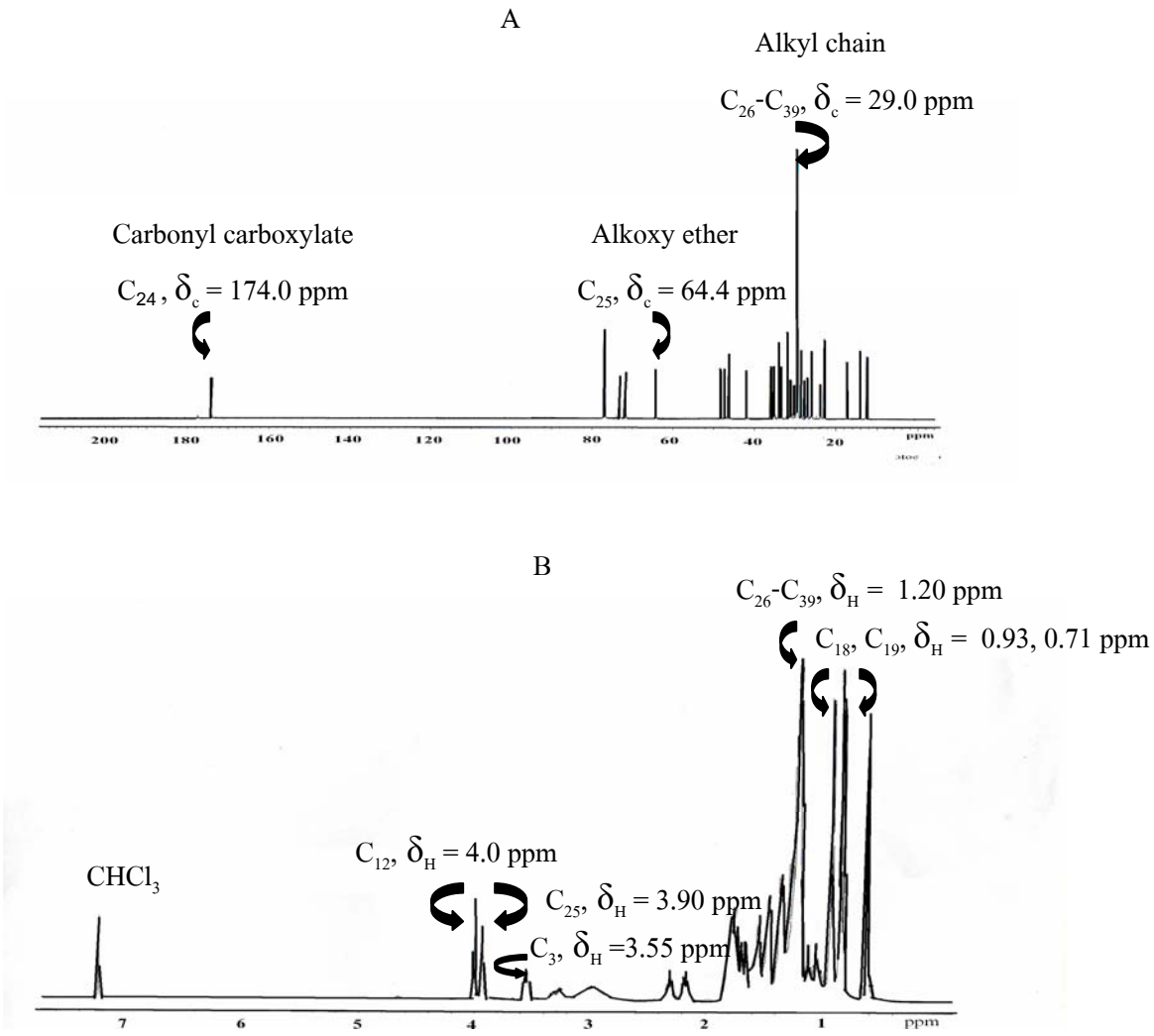

Figure 4.4 ^{13}C-NMR spectrum of CCE (A) and ^{1}H-NMR spectrum of CCE (B) ($CHCl_3$ as solvent, 500 MHz, TMS as a reference).

Table 4.1 ^{13}C and ^{1}H resonance assignment of CCE as compared with deoxycholic acid

Position	Cholate cetyl ether, $CDCL_3$ as solvent			Deoxycholic acid, $CDCL_3$ as solvent		
	Type	Carbon (ppm)	Proton (ppm)	Type	Carbon (ppm)	Proton (ppm)
1	CH_2	34.0	0.83 (d;2H)	CH_2	36.3	0.98 (d;2H)
2	CH_2	30.8	1.54 (dt;2H)	CH_2	30.9	1.59 (dt;2H)
3	CH	71.6	3.55 (dd;H)	CH	72.5	3.54 (dd;H)
4	CH_2	41.9	1.49 (dd;2H)	CH_2	37.0	1.48 (dd;2H)
5	CH	46.3	1.35 (m;H)	CH	43.5	1.39 (m;H)
6	CH_2	29.3	1.24 (dt;2H)	CH_2	28.3	1.26 (dt;2H)
7	CH_2	27.3	1.37 (dt;2H)	CH_2	27.3	1.42 (dt;2H)
8	CH	38.0	1.46 (tt;2H)	CH	37.3	1.46 (tt;2H)
9	CH	35.1	1.81 (m;H)	CH	34.6	1.89 (m;H)
10	C	35.9	-	C	35.3	-
11	CH_2	28.5	1.54 (dd;2H)	CH_2	29.8	1.53 (dd;2H)
12	CH	76.7	4.00 (t; H)	CH	74.0	3.90 (t;H)
13	C	47.1	-	C	44.8	-
14	CH	46.4	1.62 (m;H)	CH	49.1	1.62 (m;H)
15	CH_2	23.6	1.67 (dt;2H)	CH_2	24.8	1.62 (dt;H)
16	CH_2	26.0	1.29 (dt;2H)	CH_2	28.5	1.29 (dt;2H)
17	CH	49.9	1.81 (tt;3H)	CH	48.0	1.87 (dt;2H)
18	CH_3	12.6	0.70 (m;3H)	CH_3	13.2	0.71 (m;3H)
19	CH_3	17.1	0.91 (m;3H)	CH_3	17.5	0.93 (m;3H)
20	CH	35.1	1.42 (m;2H)	CH	36.6	1.42 (m;3H)
21	CH_3	22.6	0.97 (d;3H)	CH_3	23.7	1.01 (d;2H)
22	CH_2	31.8	1.34 (dt;2H)	CH_2	32.2	1.35 (s;3H)
23	CH_2	31.3	2.20 (t;2H)	CH_2	32.0	2.23 (dt;2H)
24	C	174.3	-	C	178.0	-
25	CH_2	64.4	3.90 (t;H)			
26	CH_2	30.4	1.20 (m;2H)			
27	CH_2	29.2	1.20 (m;2H)			
28	CH_2	29.2	1.20 (m;2H)			
29	CH_2	29.2	1.20 (m;2H)			
30	CH_2	29.2	1.20 (m;2H)			
31	CH_2	29.2	1.20 (m;2H)			
32	CH_2	29.2	1.20 (m;2H)			
33	CH_2	29.2	1.20 (m;2H)			
34	CH_2	29.2	1.20 (m;2H)			
35	CH_2	29.2	1.20 (m;2H)			
36	CH_2	29.2	1.20 (m;2H)			
37	CH_2	29.2	1.20 (m;2H)			
38	CH_2	29.2	1.20 (m;2H)			
39	CH_2	23.9	1.20 (m;2H)			
40	CH_3	14.0	0.83 (m;3H)			

Note: Chemical shift of ^{13}C and ^{1}H of deoxycholic acid was obtained from Vincent *et al*., 1985.

4.1.2.3 ESI-MS analysis

The chemical structure of CCE comprises of three parts; a steroid planar nucleus, hydrocarbon chains from the alkyl cahain and the ether linkage. The mass spectrum (ESI-MS) contains a base peak at 639 m/z. However, the molecular weight of CCE was not observed at 616 m/z, instead the molecule was associated with Na^+ in the matrix. Thus, the molecular ion peak could be detected at 639 instead of at 616 m/z as shown in Figure 4.5.

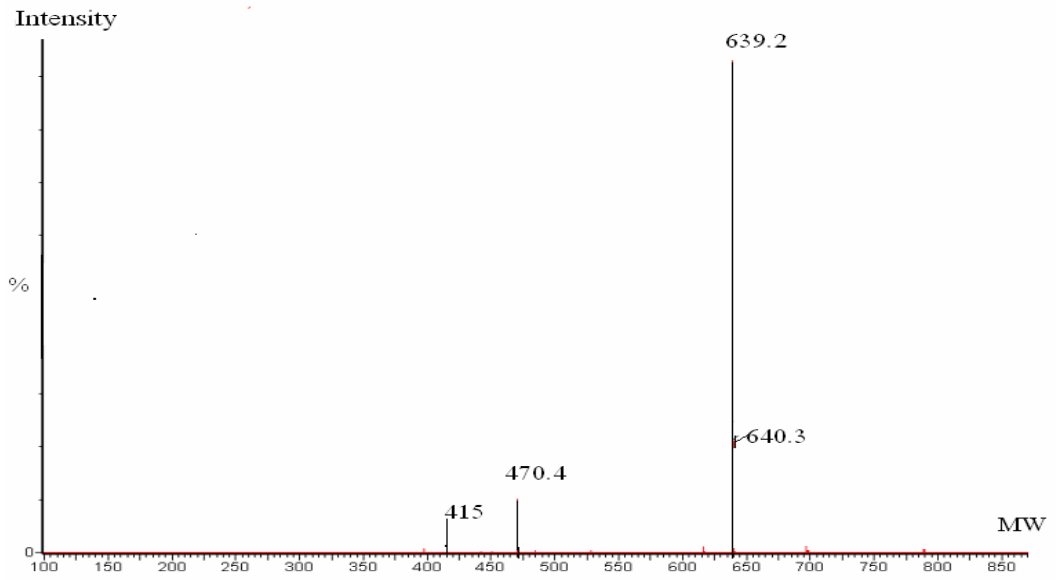

Figure 4.5 Mass spectrum of CCE

However, the rearrangement of each fragmentation, the base peak of CCE was observed at 639 m/z. The hydrocarbon chain fragmentations were located at 470 and 415 m/z. Alkyl chain was cleavaged which corresponded to loss of dodecyl ion ($C_{12}H_{25}^+$, MW = 169) as shown in Figure 4.6 A and hexadecyl ion ($C_{16}H_{33}^+$, MW = 225) as shown in Fig 4.6 B. Therfore, other two fragments were obtained at 470, 415 m/z, respectively.

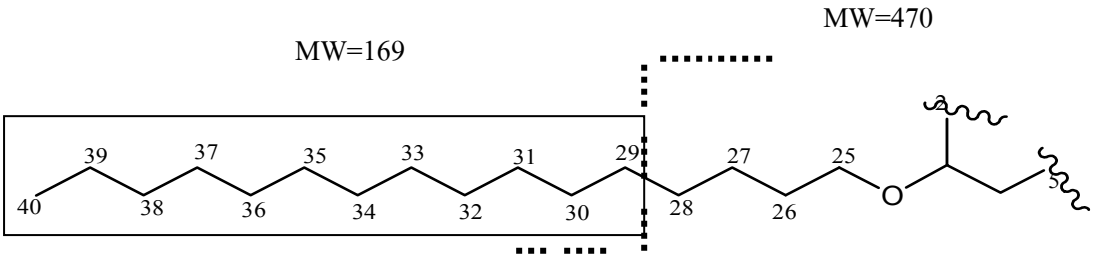

(A) Dodecyl ion ($C_{12}H_{25}^{+}$), MW = 169

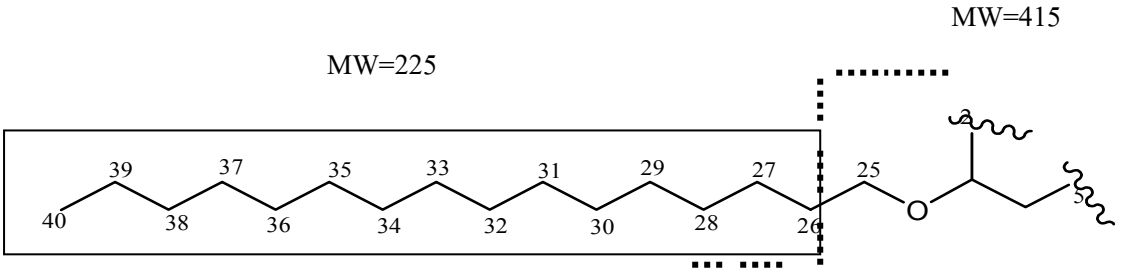

(B) Hexadecyl ion ($C_{16}H_{33}^{+}$), MW = 225

Figure 4.6 Fragmentation of hydrocarbon chain in CCE molecule

4.1.2.4 DSC and XRD analysis

DSC is useful tool to study thermal property of compound. CCE shows 100% of amorphous form at room temperature (25 °C). From the cooling curve of thermogram it was found that there were two exothermic peaks at 6.7 and 17.7 °C (Figure 4.7). This proves that CCE has liquid crystal properties at temperature lower than 20 °C. CCE gave mesophase property at temperature higher than 25 °C. X-ray diffraction (Figure 4.8) shows an amorphous form at the room temperature. The crystalline form of CCE cannot be detected because X-ray diffraction gave only one broad peak. According to DSC and XRD results, it can be confirmed that CCE is an amorphous material room at temperature (25 °C).

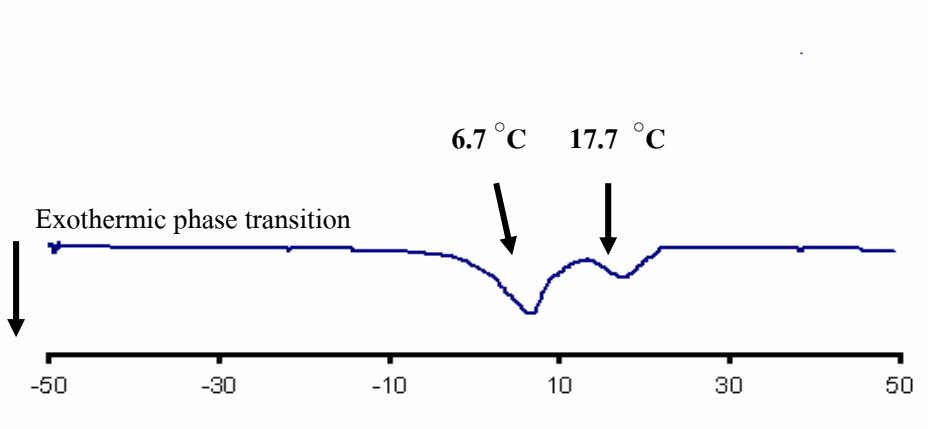

Figure 4.7 The cooling curve DSC thermogram of CCE

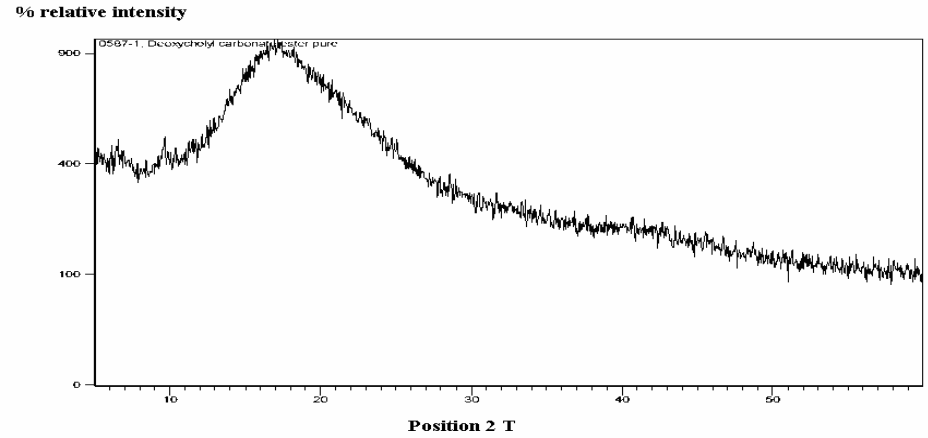

Figure 4.8 X-ray diffraction of CCE

4.2 Stability testing of pure AmB, AmB in liquid crystal

4.2.1 HPLC of AmB in liquid crystal

The analysis of free AmB by HPLC in liquid crystal is shown in Figure 4.9. The retention time for AmB was 14 min. The method exhibited linearity over the range 0.2-1.0 µg/ml

(r^2 = 0.9990). The % RSD of AmB analysis was less than 2 % in all concentrations in this study. However, the interested peak of AmB in in liquid crystal at retention time of 14 min was unable to quantify when the concentration of AmB was less than 13 ng/ml.

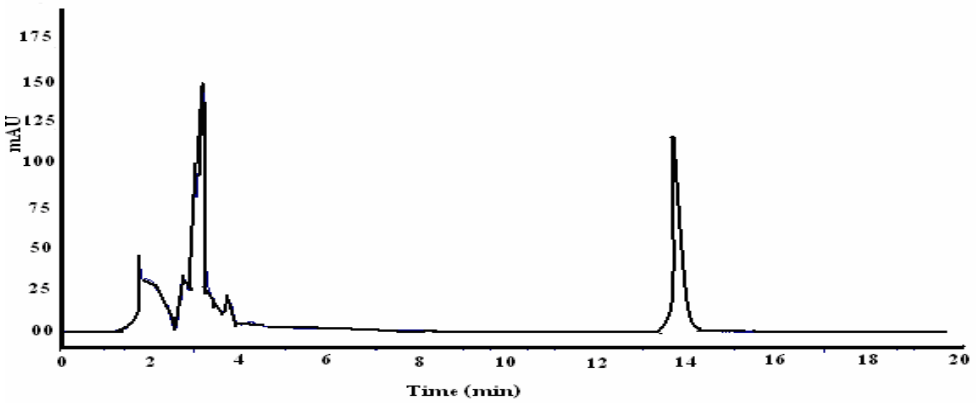

Figure 4.9 HPLC chromatograms of free AmB standard analysis

4.2.2 Content of AmB in liquid crystal

The AmB content in liquid crystal is shown in Table 4.2. It is shown that free AmB in CCE system was unable to detect. If the free drug was found at limit of quantification (13 ng/ml) or in other words it can say that free drug would be 1.3 %. Therefore, maximum encapsulation would be 98.7%. It can be postulated that AmB was incorporated completely into CCE liquid crystal. Free AmB was found to be 4.6% and 16.9 % in case of DCA and COC, respectively. Hence, % encapsulation of AmB into DCA, COC nanosystem was 95.3, 83.0, respectively. COC gave the least % encapsulated in comparison with either CCE or DCA. The least soluble properties of COC in water may be responsible for lower encapsulation because its molecules

tend to stay together rather with AmB. This suggests that the type of liquid crystal affects on % AmB encapsulation. Apart from size and functional group, affinity of liquid crystal with AmB is expected to involve zetapotential of AmB in liquid crystal nanosystem. This will be discussed later in section 4.2.4.

Table 4.2 Free AmB and AmB in different liquid crystals when AmB to liquid crystal at molar ratio 1:1 and AmB was at 1 μg/ml (Mean ± SD, n=6) by HPLC

Formulation	% Average free drug	% Encapsulation
AmB in DCA	4.6 ± 2.4	95.3
AmB in CCE	UD	98.7
AmB in COC	16.9 ± 1.6	83.0

UD = Undetected

4.2.3 Chemical stability of pure AmB and AmB in liquid crystal

According to UV spectrum of pure AmB, AmB monomer has 4 peaks with maxima at 350, 368, 388, and 412 nm. When the AmB solutions was dispersed in aqueous medium for 5 days, the spectrum shifted to shorter wavelength at 328 nm accompanied by other peaks at 365, 385 and 410 nm with decreasing intensity. This was explained by an aggregated state of AmB (Gruszecski *et al*., 2003). It can be sure that AmB formed aggregation to be a dimer at 8 days as shown in

Figure 4.10 A. UV band shifted to locate at 320 nm while the spectra of AmB in CCE and COC did not change significity as shown in Figure 4.10 B & C, respectively. The spectrum represented that AmB in CCE and COC was expected to be in a monomer within 14 days. Pure AmB has shorter stability than AmB in CCE and COC. It is believed that liquid crystal can protect AmB from self aggregation and expected that either COC or CCE can form nanosystem. In addition, AmB in CCE was more stable than AmB in COC. When the structures of COC and CCE were compared, it reveals that COC has a larger structure than CCE and it is less soluble in water. Moreover, COC has one double bond between C_{17}-C_{18} so the stability of COC is expected to be less than that of CCE.

4.2.4 Size stability of pure AmB and AmB in liquid crystal

The size stability of pure AmB, AmB in liquid crystals was determinined by PCS as shown in Figure 4.11. The PCS showed that pure AmB was unstable nanosystem with size around 600 nm. After 6 days, the size was increased significantly to 4998 nm. When the AmB in CCE (1:1) at 10 μg/ml was dispersed in aqueous solution, it formed a nanosystem with size of 243 nm. It was stable for more than 15 days. While COC formed a larger AmB in nanosystem with a size of 695 nm, it maintained this size for 10 days. After that, the size containing COC was increased significantly from 695 nm to 3110 nm. Due to its structure, CCE has polar contributing from hydroxyl groups as compared with COC. The size stability of COC system was lost after 10 days as it aggregated. The size was found to be in micron size. AmB-COC has better size stability

than pure AmB. Thus, it proved that the liquid crystal can protect AmB from monomer to be dimer or aggregate system.

One hypothesis of AmB aggregate is due to a negative zeta potential (-19 mV) at pH 6.25 as shown in Table 4.3. Since the pK_a value of the amino group and carboxyl group are 10 and 5.7, respectively. AmB in CCE and COC had a negative zetapotential (-12.2, -36.4 mv) from carboxylic group and carbonyl carbonate, respectively. The interactions between CCE or COC with AmB would be essentially hydrophobic and vander waals forces rather than electrostatic interactions. However, AmB in CCE showed an increase in the zeta potential less than AmB in COC. Theoretically, the stable nanosystem should have zeta potential about -20 mv. In this case it is rather surprise when we consider size stability with zeta potential and found that AmB in COC was less stable than AmB in CCE. Therefore the stability AmB in CCE is not only zeta potential factor but also the size of the system. It is rather difficult to conclude about the nature of the interaction between AmB and liquid crystal using only zeta potential data.

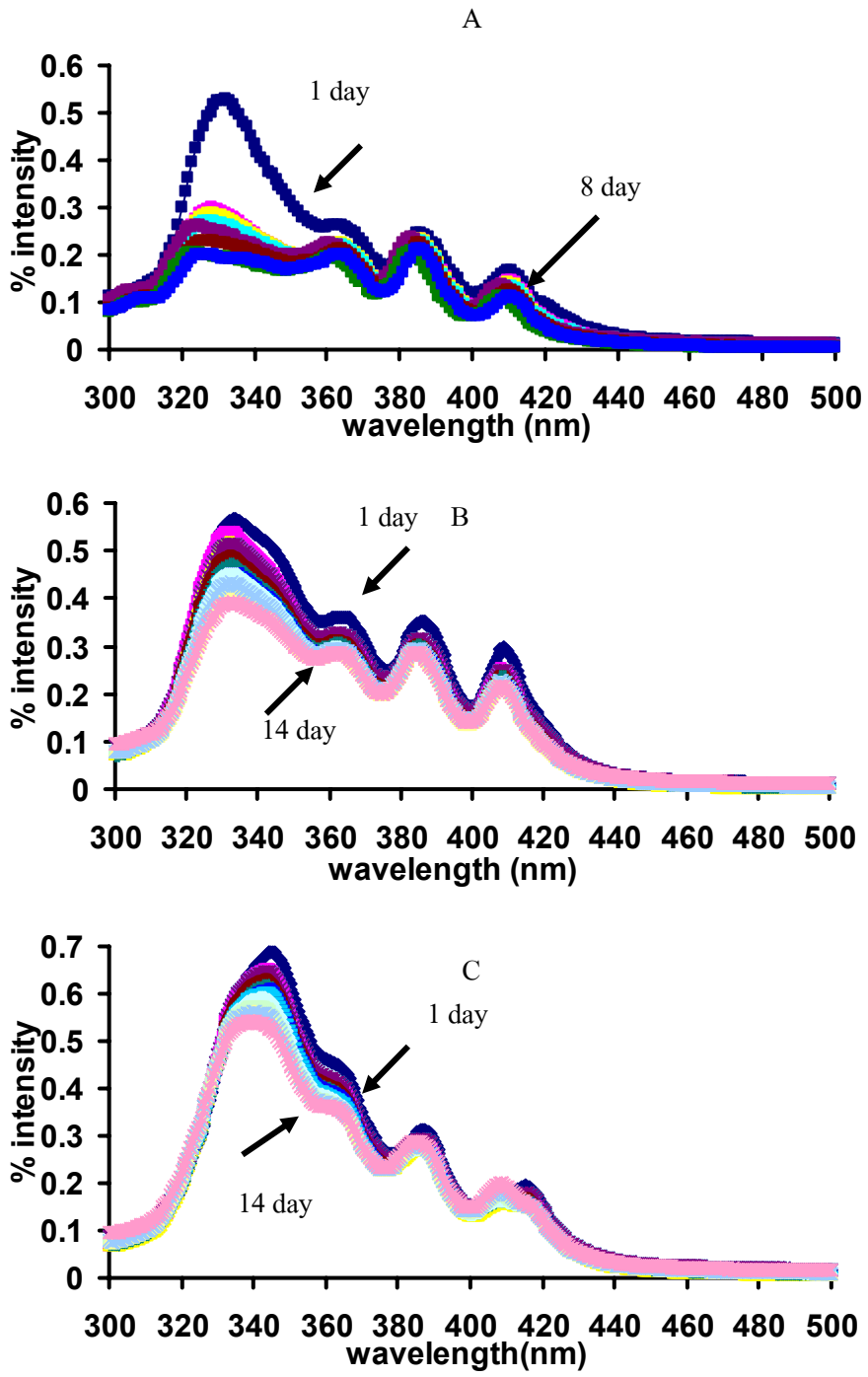

Figure 4.10 UV spectrums of AmB 100 µg/ml (A), AmB-COC (B), AmB-CCE (C) aqueous solution during 14 days

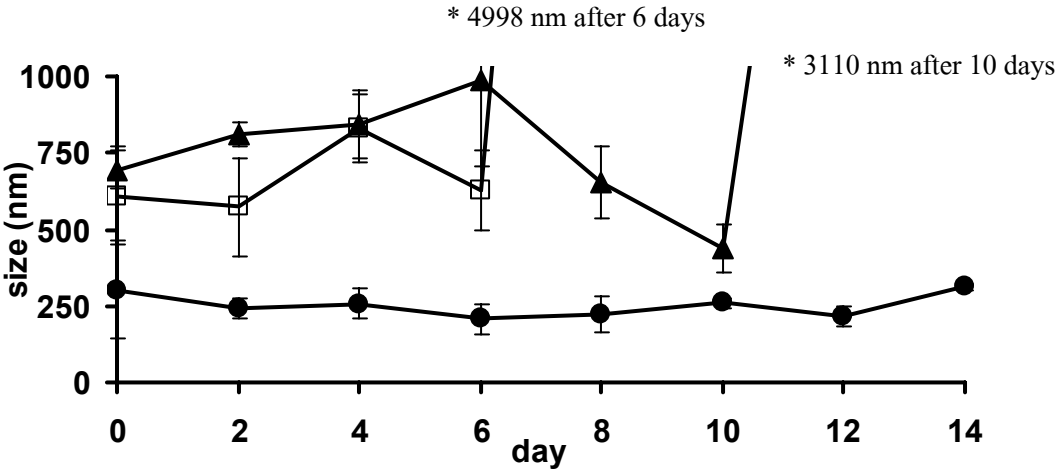

Figure 4.11 Size stability of pure AmB (10 μg/ml) in the aqueous solution (□), AmB-COC (▲), AmB- CCE (●) during 14 day (mean ± SD, n=3).

Table 4.3 Zetapotential of pure AmB (1 μg/ml) and AmB in liquid crystal system

Formulation	Zeta potential (mV)
AmB	-19 ± 1.1
COC	-23.2 ± 0.6
CCE	-8.6 ± 0.5
AmB in COC	-36.4 ± 0.2
AmB in CCE	-12.2 ± 1.0

4.3 Microbial assay of pure AmB and AmB in liquid crystal

4.3.1 Potency of pure AmB and AmB in liquid crystal

In this triplicate of experimental design, using three dose levels for each standard and sample was tested as following the procedure described in the USP 24 NF19. The zone diameter is shown in Figure 4.12. The calibration curves of this experiment, constructed by plotting of zone diameter (mm) versus concentrations (μg/ml) showed good linearity (R^2 = 0.9539). The representative linear equation for reference solutions was Y = 0.2748X-4.7696, where X is the zone diameter and Y the concentration of AmB. The calculation procedure usually assumes a direct relationship between the observed zone diameter and the applied dose. The corresponding mean zone diameters for reference solutions were 19.47, 20.39, 21.24, 22.29, 22.51 mm for 0.6, 0.8, 1, 1.2, 1.5 μg/ml, respectively. While the zone diameter for AmB in liquid crystal were 21.4, 21.97, 22.02 mm for AmB in COC, AmB in DCA, AmB in CCE, respectively. The % quantification of AmB in liquid crystal was 96, 110, 112 % for AmB in COC, DCA, CCE, for respectively. AmB has potency in range 90-120 of the percentage labeled amount. The quantification of AmB in liquid crystal was not significantly different from AmB reference. Hence, CCE, COC, DCA did not affect the potency of AmB.

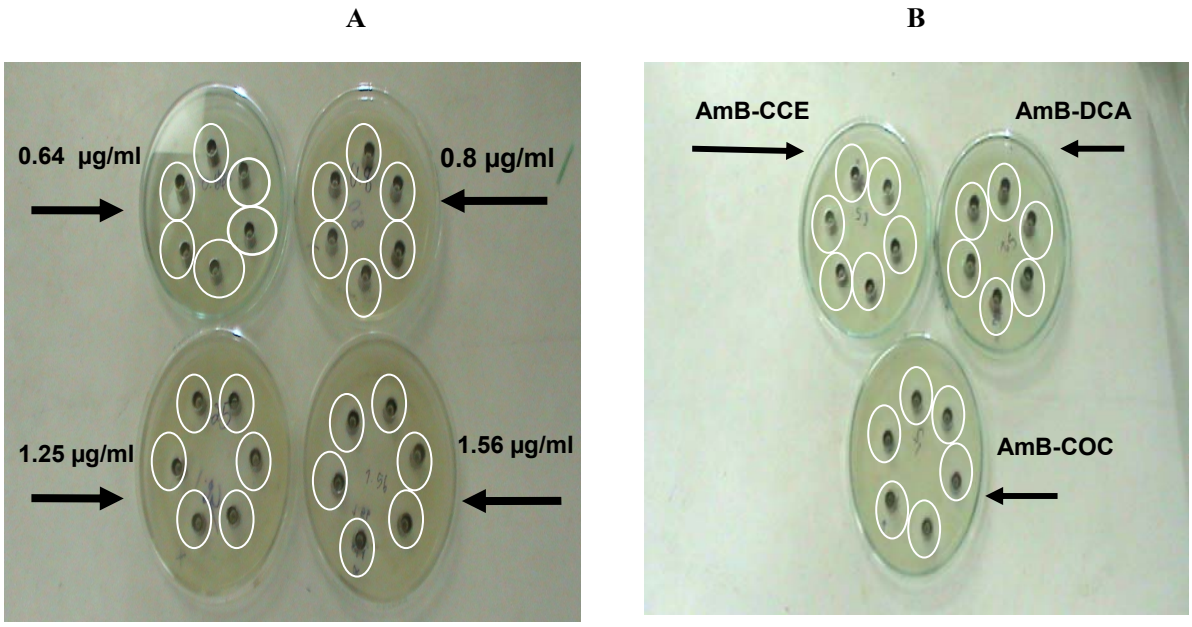

Figure 4.12 Photographs of the zone diameter for AmB standard (A) and AmB in liquid crystal (B). Clear zones were redrawn.

4.3.2 Susceptibility testing of *C. neoformans* by broth microdilution analysis

The MICs obtained for pure AmB, AmB in liquid crystal (DCA, COC, CCE) against *C. neoformans* were covered range to those reported previously (as shown in Table 4.4). MICs range of AmB against *C. neoformans* was previously reported to be 0.25-1 µg/ml (NCCL, 2007), 0.03-1.0 µg/ml (Weerawat, 2006). The AmB in CCE gave the lowest MICs and was 2-4 times lower than pure AmB (0.125 µg /ml). The lower MIC of AmB in liquid crystal suggests that AmB in liquid crystal have a synergic effect because the liquid crystal cannot inhibit *C. neoformans* by itself. MICs of pure liquid crystal were more than 16 µg/ml. AmB in liquid may possibly form inophores thus enhance AmB permeability into fungal membrane (Umgawa, 1984).

Table 4.4 MICs of *C. neoformans* for pure AmB, pure liquid crystal and AmB in CCE by broth microdilution analysis

Drug	**MIC (µg/ml)**
AmB	0.125
DCA	> 16
COC	> 16
CCE	> 16
AmB in DCA	0.0625
AmB in COC	0.125
AmB in CCE	< 0.031

4.4 Cytotoxicity of pure AmB and AmB in liquid crystal

4.4.1 Hemolysis of pure AmB and AmB in liquid crystal

From Figure 4.13 (A, B), the hemolysis of AmB in liquid crystal was carried out at various concentrations and times. The hemolysis of AmB in three liquid crystals were determined at a concentrations of 10, 5, 1 μg/ml, respectively. The hemolysis shows that the AmB in liquid crystal with molar ratio 1:1 at concentration 1 μg/ml was less erythrocyte lysis (3%) at 6 h while the AmB in three liquid crystals showed differently hemolysis activity at molar ratio with 1:1. It was shown that the hemolysis of AmB in DCA reached 35 % in 24 h. However, the % of hemolysis of AmB in liquid crystal was less than pure AmB or pure liquid crystal, while AmB in COC and CCE showed drastically low hemolysis. The AmB in COC and CCE with molar ratio 1:1 at concentration 1 μg/ml was slightly less hemolysis. The hemolysis of AmB in COC and CCE was 0, 1, 5 % at 0, 3, 6 h, indicating that the AmB that release of AmB in COC and CCE was slow. The less of hemolysis activity may also reflect the release of monomeric AmB in CCE as opposed to pure AmB or AmB in DCA that releases both aggregated and monomeric forms of AmB. However, it is known that monomeric AmB caused less hemolysis effect than the aggregated forms of the AmB. When the RBC was observed under light microscope, it is clearly shown the difference between non hemolytic RBC and lysed RBC (Figure 4.14).

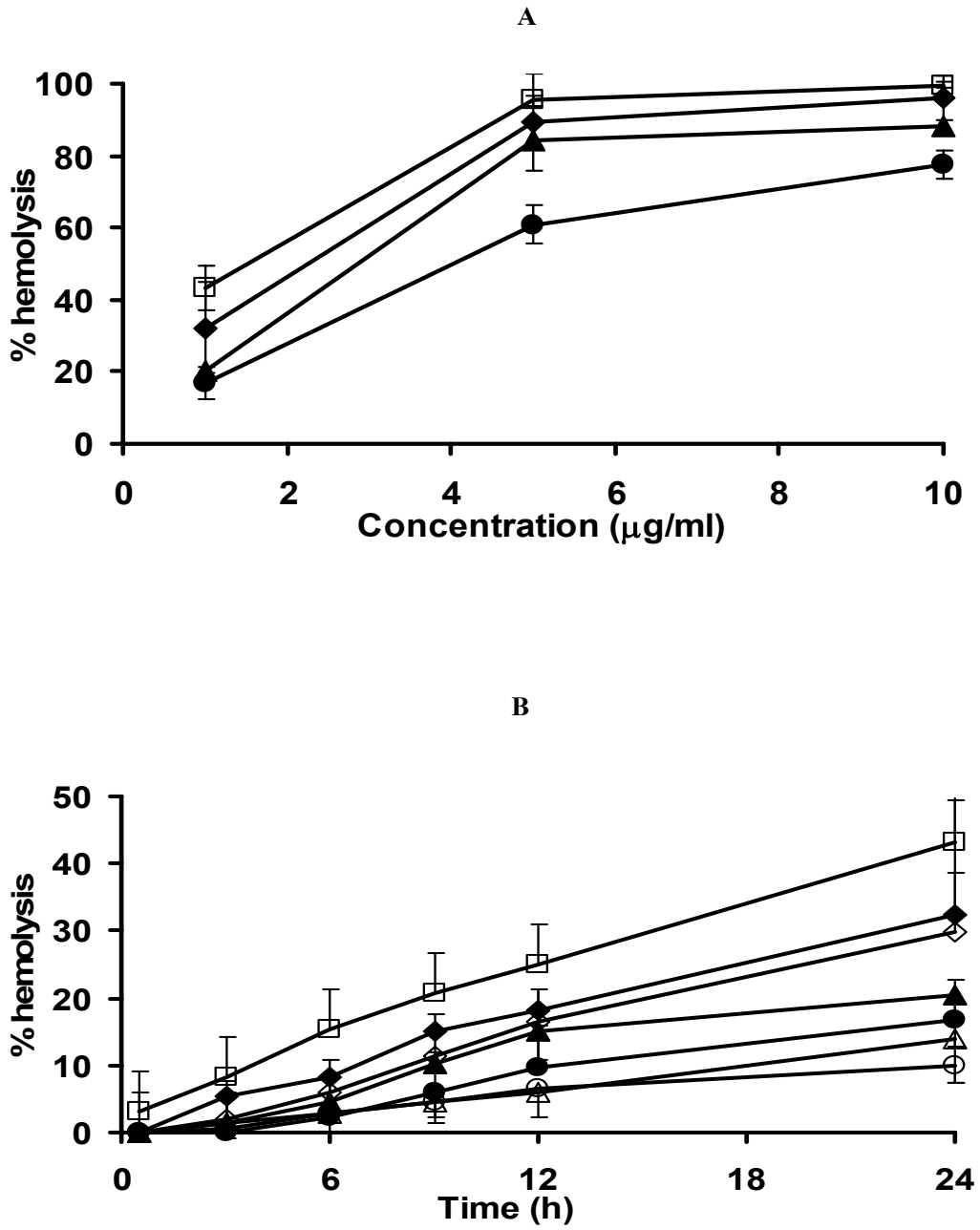

Figure 4.13 Concentration dependent hemolysis profile of pure AmB (□), AmB in DCA (♦), AmB in COC (▲) and AmB in CCE (●) as shown in (A) and time dependent hemolysis profile of pure AmB (□), AmB in DCA (♦), AmB in COC (▲), AmB in CCE (●), pure DCA (◊), pure COC (△) and pure CCE (○) as shown in (B)

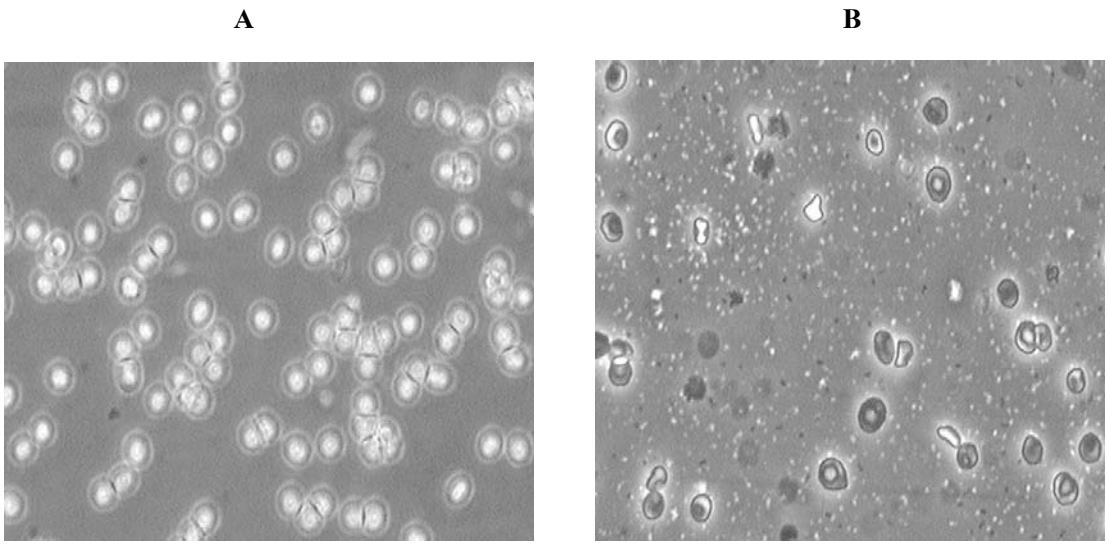

Figure 4.14 RBC observed under light microscope at magnification 200; non hemolytic RBC (A) and lysed RBC (B)

4.4.2 Cytotoxicity of pure AmB, pure liquid crystal and AmB in liquid crystal with monocyte and alveolar macrophage

For the cytotoxicity test with J 774.2 and NR 8383 cell line of pure AmB, It is shown in Figure 4.15A. The pure AmB was toxic to monocyte and macrophage cells when AmB concentration was higher than 0.1 µg/ml. The toxicity to both cells increased when the drug concentration increased. The cells survival was 8.2% at a concentration of 100 µg/ml. When the concentration of AmB was decreased to be 10 µg/ml, % cell survival increased to 40 and 58 for monocyte and macrophage cell, respectively. LD_{50} of monocyte and macrophage were found to be 2.8 and 1 µg/ml, respectively. The viabilities of monocyte and macrophage after incubation with CCE, COC and DCA are shown in Figure. 4.15 B & C. It was evident that CCE, DCA, COC and were not toxic to monocyte and macrophage cell line at a concentration less than 60 µg/ml.

The % viability of monocyte cell line incubated with CCE reached 100% at all concentrations used in this study. Pure DCA is also not toxic to monocyte although the % viability of cell was less than that of CCE. Whereas, COC gave the least % viability especially at a concentration higher than 100 µg/ml. The macrophage cell line gave almost similar results with monocyte cell line, However, it was found that the % viability of macrophage cell line was less than that of the monocyte cell line. CCE, DCA and COC were not toxic to macrophage cell at a concentration less than 60 µg/ml. When the concentration was increased more than 60 µg/ml, the % viability in case of DCA and COC decreased significantly. It can be concluded that CCE with AmB was the safest nanosystem in this study.Thus we expect that CCE can be applied to form micelle with AmB with least affecting monocyte and macrophage cell line.

The AmB 100 µg/ml in CCE, DCA, and COC showed more toxic to cell line than pure liquid crystals. However, the results found that AmB 100 µg/ml in CCE gave the highest % viability following by AmB 100 µg/ml in DCA and AmB 100 µg/ml in COC as shown in Figure 4.16A. The % viability of monocyte cell line in AmB 100 µg/ml in CCE, AmB 100 µg/ml in DCA and AmB 100 µg/ml in COC were 20, 15 and 10, respectively. On the other hands, the % viability of CCE, DCA, and COC were not significantly different at all concentrations. In addition, the liquid crystal can form micelle with some amount of AmB, so the % viability of AmB with liquid crystal is higher than the % viability of pure AmB. While the % viability of macrophage cell line in AmB 100 µg/ml in CCE, AmB 100 µg/ml in DCA, and AmB 100 µg/ml in COC were 10-20, 5-10 and 4-5 as shown in Figure 4.16B. Moreover, the results revealed that

% viability of macrophage cell line was less than % viability monocyte cell line. When the concentration of AmB was decreased to 10 µg/ml, the % viability increased. The viability of monocyte cell line in AmB in CCE was 80-100 %, AmB in DCA was 70- 80 % and AmB in COC was 60-80 % as shown in Figure 4.16C. While the viability of macrophage cell line in AmB in CCE, AmB in DCA and AmB in COC were 40-100%, 20-80% and 10-60%, respectively (Figure 4.16D). It is important to note was noted that the AmB is the safest with CCE because the 10 µg/ml with liquid crystal the highest survival was obtained while the DCA and COC gave almost similar results. It was concluded that liquid crystal together with AmB decrease toxicity of AmB. Although, the % viability of AmB 10 µg/ml with liquid crystal for monocyte cell line was higher than the pure AmB but the % viability of AmB in DCA, AmB in COC for macrophage was lesser than % viability of AmB in DCA, AmB in COC for monocyte at concentration at 140-180 µg/ml. It might prove that liquid crystal cause toxicity in macrophage cell line more than monocyte cell line.

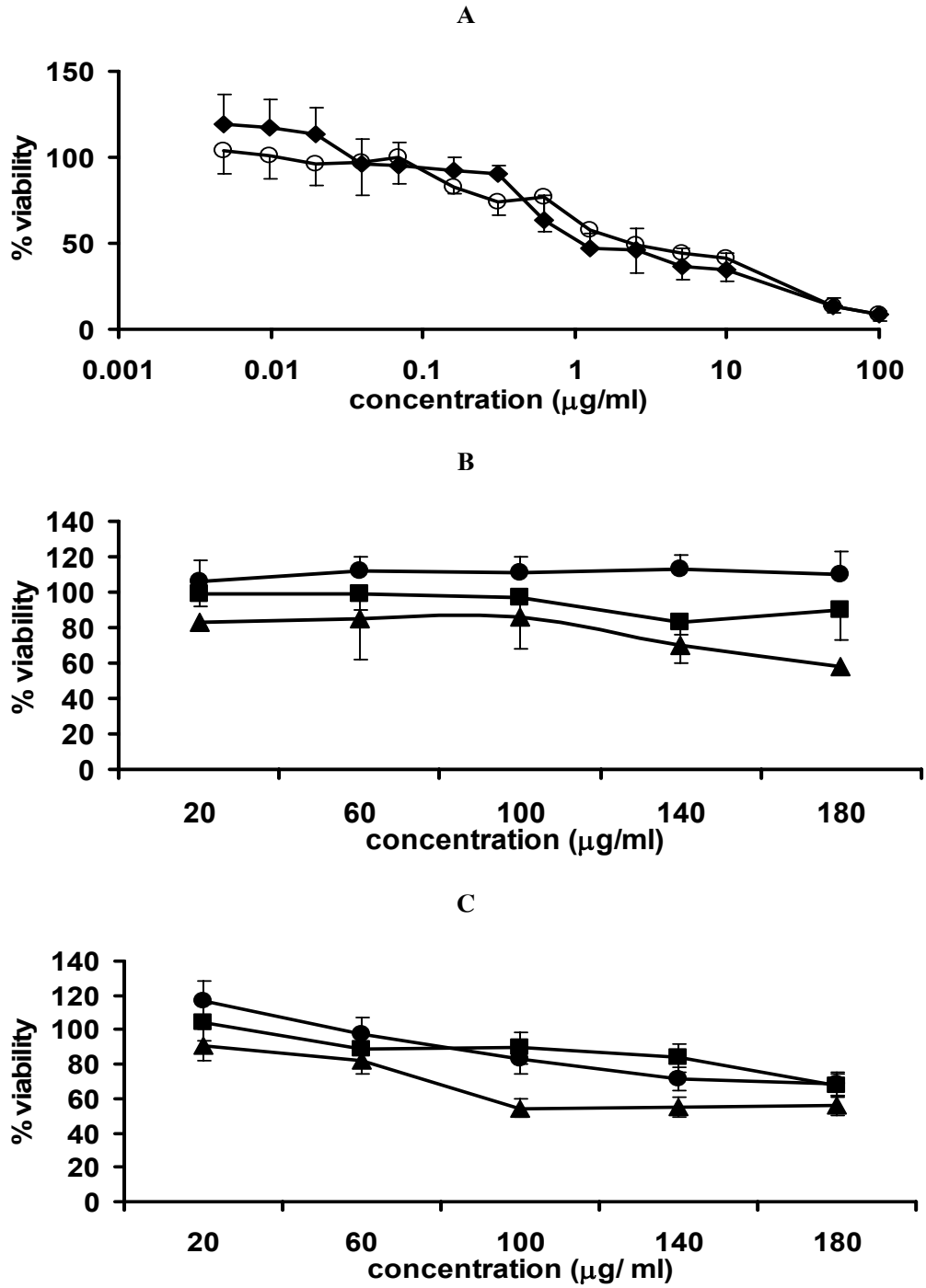

Figure 4.15 The % viability of monocyte J 774.2 cell line (◆) and macrophage NR 8383 cell line (○) after incubation with pure AmB (A), The % viability of monocyte J 774.2 cell line (B) and macrophage NR 8383 cell line (C) after incubation with CCE (●), DCA (■) and COC (▲)

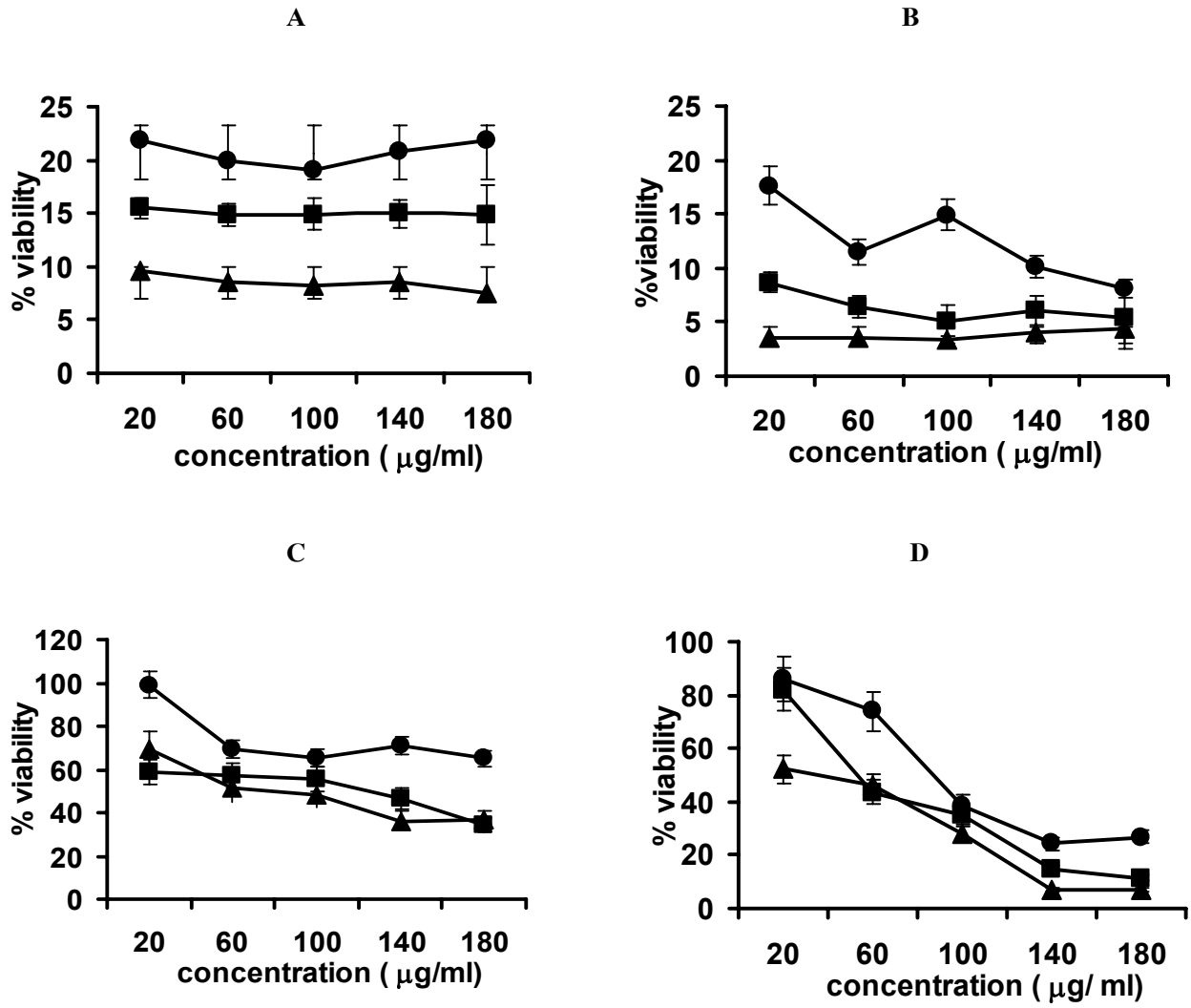

Figure 4.16 The % viability of monocyte J 774.2 cell line (A), macrophage NR 8383 cell line after incubation with AmB 100 μg/ml in CCE, DCA, COC (B) and the % viability of monocyte J774.2 cell line (C), macrophage NR 8383 cell line (D) after incubation with AmB 10 μg/ml in CCE (●), DCA (■), COC (▲)

CHAPTER 5

CONCLUSIONS

The goal of thesis was to synthesis and purify new product to be able to use in nanodelivery system of AmB. In addition, the antifungal activity and toxicity of AmB in liquid crystal were evaluated in comparison with conventional AmB formulation. The data presented here show that CCE comprises of three parts; a steroid planar nucleus, hydrocarbon chains from the fatty alcohol and the ether linkage. At the room temperature, the liquid crystal is in an amorphous form. For the size and stability test, it reveals that CCE and COC liquid crystals are able to form nanodelivery system of AmB. Liquid crystals with AmB are found to be more stable than pure AmB. Especially, CCE can protect AmB changes from monomeric to dimeric form. Prolonged size stability of particles between 200-300 nm was obtained at least for fourteen days. CCE nanosystem can protect the AmB from aggregation. Perhaps, it is one of the method to minimize nephrotoxicity. In addition, it was found that AmB at 1 μg/ml was completely encapsulated in CCE. For the susceptibility test by cylinder plate method and broth microdilution analysis, it was found that CCE enhanced the activity of AmB. MICs against *C.neoformans*. AmB in CCE has a lower MICs than conventional AmB. One of the purposes of AmB in liquid crystal was to reduce AmB toxicity especially to red blood cell. The data of acute toxicity test showed that AmB in liquid crystal and pure AmB had similar results. The toxicity of AmB had been

suggested to be the effects of the aggregation of AmB. It was found that cell toxicity induced by AmB in DCA was faster than that induced by AmB in CCE. Free AmB in CCE might be release more slowly and hence lower concentration is less harmful to the RBC than the quick release of AmB from the AmB in DCA leading to the slightly delayed toxicity. From the result of cytotoxicity test, we found that the CCE was not toxic to monocyte and macrophage cell line. It can be suggested for future work that suitable formulation of AmB in CCE should be in dry powder form. This is because AmB in CCE formulation was not stable in aqueous medium. All primary data of AmB in CCE supported the evidence that AmB in CCE is a promising nanodelivery system.

BIBLIOGRAPHY

Adams, M.L. and Kwon, G.S. 2003. The effects of acyl chain length on the micelle properties of poly (ethylene oxide)- block- poly(N-hexyl-L aspartamide conjugates. *J. Control. Release.* 87, 23-32.

Anaizi, N. 2007. The drug monitor: Amphotericin B lipid complex. (http//www.thedrugmonitor.com/ABLC.html).

Antoniadou, A. and Dupont, B. 2005. Lipid formulations of AmB: where are we today?. *J. Med. Mycol.* 15, 230-238.

Baginski, M. and Borowski, E. 1997. Distribution of electrostatic potential around amphotericin B and its membrane targets. *J. Mole. Struct.* 389, 139-146.

Baginski, M., Resat, H. and Borowski, E. 2002. Comparative molecular dynamics simulations of amphotericin B-cholesterol/ergosterol membrane channels. *Biochim. Biophys. Acta.* 1567, 63-78.

Bekersky, I., Fielding, R. M., Buell, D. and Lawrence, I. 1999. Lipid-based amphotericin B formulations:from animals to man. *J. Pharm. Sci.* 2, 230-236.

Benita, S. 1996. Microencapsulation methods and industrial applications. Marcel Dekker. N.J. USA. pp 225

Binnemans, K. 2005. Ionic liquid crystal. *Chem. Rev.* 105, 4148-4204.

Brajtburg, J., Powderly, G.W., Kobayashi, S.G. and Medoff, G. 1990. Amphotericin B: current understanding of mechanism of action. *Antimicrob. Agents. Chemother.* 34, 183-188.

Caillet, J., Berges, J. and Langlet, J. 1995. Theoretical study of the self-association of AmB. *Biochim. Biophys. Acta.* 1240, 179-195.

Chavanet, P. 1997. Amphotericine B deoxycholate (Fungizone®): vieux medicament, nouvelles versions. *J. La Revue. De Med. Intern.* 18, 153-165.

Cotero, V.B., Rebolledo, A.S. and Ortega, B. I. 1998. On the role of sterol in the formation of the amphotericin B channel. *Biochim. Biophys. Acta.* 1375, 43-51.

Czub, J., Borowski, E. and Baginski, M. 2007. Interactions of amphotericin B derivatives with lipid membranes A molecular dynamics study. *Biochim. Biophys. Acta.* 1768, 2616-2626.

Cybulska, B., Bolard, J., Seksek, O, Czerwinski, A. and Borowski, E. 1995. Identification of the structural elements of amphotericin B and other polyene macrolide antibiotics of the heptaene group influencing the ionic selectivity of the permeability pathways formed in the red cell membrane. *Biochim. Biophys. Acta.* 1240, 167-178.

Dadachova, E. 2005. Ionizing radiation changes the electronic properties of melanin and enhances the growth of melanized fungi. (http://en.wikipedia.org/wiki/Cryptococcus_neoformans).

Edler, M and Uehara, J. 2007. Research develop new drug paradigm, liquid crystal pharmaceutical. (http//www.kent.edu/media/NewsReleases/LCP.cfm).

Elser, W., Pohlmann, W.L.J. and Boyd, R.P. 1973. Cholesteryl n-alkyl carbonates. *Liq. Cryst.* 20, 77-86.

Espuelas, M. S., Legrand, P., Irache, J. M., Gamazo, C., Orecchioni, A. M., Devissaguet, J. P. and Ygartua, P. 1997. Poly ([ε]-caprolactone) nanospheres as an alternative way to reduce AmB toxicity. *Int. J. Pharm.* 158, 19-27.

Friberg, S. 2000. Phase of Liquid crystal (http//plc.cwru.edu/tutorial/enhanced/files/lc/phase/phase.htm).

Fournier, I., Barwicz. J.and Tancrède, P. 1998. The structuring effects of AmB on pure and ergosterol or cholesterol-containing dipalmitoylphosphatidylcholine bilayer: a differential scanning calorimetry study. *Biochim. Biophys. Acta.* 1373, 76-86.

Gruszecki, W. I., Gagos, M. and Herec, M. 2003. Dimers of polyene antibiotic AmB detected by means of fluorescence spectroscopy: molecular organization in solution and in lipid membranes. *J. Photochem. Photobiol., B.* 69, 49-57.

Hartsel, S. and Bolard, J. 1996. Amphotericin B: new life for an old drug. *J. TiPS.* 17, 445-449.

Kimura, N.M., Campos, A., Santoro, P.A. and Simoes, M. 2007. Thermal diffusivity measurement in a lyotropic discotic nematic phase. *Phys.Lett.A*.1, 1-4.

Kintzel, P. 1993. Martindale: The extra Pharmacopia. Reynolds, E. F. J (ed.) Amphotericin B. The Pharmaceutical Press, Lambeth High street, London, UK. pp. 315-319.

Lambros, M.P., Abbas, S.A. and Bournw, D.W.A. 1996. New high-performance liquid chromatrographic method for Amphotericin B analysis using an internal standard. *Chromatogr. Sci*. 685, 135-140.

Larabi, M., Gulik, A., Dedieu, J.-P., Legrand, P., Barratt, G. and Cheron, M. 2004. New lipid formulation of amphotericin B:spectral and microscopic analysis. *Biochim. Biophys. Acta.* 1664**,** 172-181.

Legrand, P., Romero, E.A., Cohen, E., Bolard, J. 1992. Effects of aggregations and solvents on the toxicity of amphotericin B to human erythrocytes. *Antimicrob. Agents. Chemother.* 36(11), 2518-2522.

Lin, Y. Y., Chen, K. S and Lin, Y.S. 1996. Development and investigation of a thermo-responsive cholesteryl oleyl carbonate-embedded membrane. *J. Control. Release.* 41, 163-170.

Lin, Y. S., Ho, J.C and Li, J.M. 2001. Precision and reproducibility of temperature response of a thermo-responsive membrane embedded by binary liquid crystal for drug delivery. *J. Control. Release*. 73, 293-301.

Lin, Y. S., Tseng, H.Y and Li, J.M. 2000. Phase studies and thermal stability of binary systems of cholesteric liquid crystal. *Appl. Phys. A*. 70, 663-668.

Matsumori, N., Eiraku, N., Matsuoka, S., Oishi, T., Murata, M., Aoki, T. and Ide, T. 2004. An amphotericin B-ergosterol covalent conjugate with powerful membrane permeabilizing activity. *Chem. Biol.* 11**,** 673-679.

Mazerski, J. and Borowski, E. 1996. Molecular dynamics of AmB. II. dimer in water. *J. Biophys. Chem.* 57, 205-217.

Mehta, R., Lopez, B. G., Hopfer, R., Mills, K. and Juliano, R. L. 1984. Liposomal AmB is toxic to fungal cells but not to mammalian cells. *Biochim. Biophys. Acta.* 770, 230-234.

Mcginnis, R. M and Rinaldi, G.M. 1991. Antibiotics in laboratory Medicine. Lorian, V (ed.) Antifungal drug: mechanism of action, drug reistance, susceptibility and assay of activity in biological fluids. Williams and Wilkins, Baltimore, Maryland*,* USA. pp. 198-243.

Nesseem, I.D. 2001. Formulation and evaluation of itraconazole via liquid crystal for topical delivery system. *J. Pharm. Biomed. Anal.* 26, 387-399.

Nooney, L., Matthews, C. R. and Burnie, P.J. 2005. Evaluation of mycograb®, amphotericin B, caspofungin, and fluconazole in combination against *Cryptococcus neoformans* by checkerboard and time-kill methodologies. *Diagn. Microbiol. Infect. Dis.* 51, 19-29.

Robinson, R.F. and Nahata, M. 1999. A comparative review of conventional and lipid formulations of AmB. *Clin. Pharmacol. Ther.* 24, 249-257.

Romanini, D., Avalle, G., Nerli, B. and Pico, G. 1999. Thermodynamic and spectroscopic features of the behavior of amphotericin B in aqueous medium. *J. Biophys. Chem.* 77, 69-77.

Russell, E. 2007. Antifungal pharmacology. (http//www. Doctorfungus.org/thedrugs /antif_pharm.html).

Saeva, F.D. 1979. Liquid crystals: The fourth state of matter. Marcel Dekker, N.J, USA. pp 286-300.

Salunke, B.D., Hazra, G.B and Pore, S.V. 2003. Bile acid–polyamine conjugates as synthetic ionophores. ARKIVOC, Pune, India. pp.115-125.

Sedlak, M., Pravda, M., Kubicova, L., Mikulcikova, P. and Ventura, K. 2007. Synthesis and characterization of a new pH-sensitive Amphotericin B-poly (ethylene glycol)-b-poly (l-lysine) conjugate. *Bioorgan. Med. Chem. Lett.* 17, 2554-2557.

Silberstein, A. 1998. Conformational Analysis of amphotericin B-cholesterol channel complex. *J. Mem. Biol.* 162**,** 117-126.

Stadler, E., Dedek, P., Yamashita, K. and Regan, S. L. 1994. Amphotericin B mimics: a sterol ionophore. *J. Am. Chem.Soc.* 116, 6677-6682.

Susan, B., Ann, S, Patricia, E. H. and Joanne F. K. 1996. The Merck Index. Susan, B (ed.). Amphotericin B. Merck research laboratories division of merck & CO., Inc. whitehouse, N.J, USA. pp. 628.

Takakazu, O. and Mohammad, A.H. 1998. In vitro and in vivo activities of ns-718, a new lipid nanosphere incorporating amphotericin B against *Aspergillus fumigatus*. *Antimicrob. Agents. Chemother*. 471-475.

Therese, K.L. Bagyalakshmi, R., Madhavan, H.N. and Deepa, P. 2006. In vitro susceptibility testing by agar dilution method to determine the minimum inhibitory concentrations of amphotericin B, fluconazole and ketoconazole against ocular fungal isolates. *J. Indian. Microbiol.* 24(4)**,** 273-279.

Tiyaboonchai, W. and Limpeanchob, N. 2007. Formulation and characterization of amphotericin B-chitosan-dextran sulfate nanoparticles. *Int. J. Pharm.* 329**,** 142-149.

Umegawa, Y., Matsumori, N., Oishi, T. and Murata, M. 2007. Amphotericin B covalent dimers with carbonyl-amino linkage: a new probe for investigating ion channel assemblies. *Tetrahedron lett*. 48, 3393-3396.

Urbina, J. A., Pekerar, S., Le, H.-B., Patterson, J., Montez, B. and Oldfield, E. 1995. Molecular order and dynamics of phosphatidylcholine bilayer membranes in the presence of cholesterol, ergosterol and lanosterol: a comparative study using 2H-, 13C- and 31P-NMR spectroscopy. *Biochim. Biophys. Acta.* 1238, 163-176.

US Pharmacoepia 24 NF 19. 2000. US Pharmacoepia Convention, Inc., Rockville, MD, USA. pp 138-139.

Vincent, D., Barnes, S. and Muccio, D. 1985. Nuclear magenetic resonance spectroscopy of bile acids. Development of two-dimensional NMR methods for the elucidation of proton resonance assignments for five common hydroxylayed bile acids, and their parent bile acid, 5b-cholanoic acid. *J. Lipid. Res.* 26, 1068-1078.

Weerawat, M. and Supeda, T. 2006. Antifungal susceptibilities of C*ryptococcus neoformans* cerebrospinal fluid isolates and clinical outcomes of crytococcal meningitis in HIV-infected patients with/without fluconazole prophylaxis. *J. Med. Assoc. Thai.* 89, 795-801.

Wong-Beringer, A., Jacob, R.A and Guglielmo, B. 1998. Lipid formulations of amphotericin B: clinical efficacy and toxicities. *Clin. Infect. Dis*. 27.603-618.

Yu, B. G., Okano, T., Kataoka, K. and Kwon, G. 1998. Polymeric micelles for drug delivery: solubilization and haemolytic activity of AmB. *J. Control. Release.* 53, 131-136.

Zhu, X. X. and Nichifor, M. 2002. Polymeric Materials Containing Bile acids. *Acc. Chem. Res*. 35, 539-546.

APPENDIX

APPENDIX

CHEMICAL COMPOUNDS

1. AMPHOTERICIN B

Commercial name: Ambisome; Amphozone; Fungizone; Fungilin; Amphotec

Chemical name:

(1R(1R*,3S*,5R*,6R*,9R*,11R*,15S*,16R*,17R*,18S*,19E,21E,23E, 25E,27E,29E,31E,33R*,35S*,36R*,37S*))-33-((3-Amino-3,6-dideoxy-beta-D-mannopyranosyl)oxy)-1,3,5,6,9,11,17,37-octahydroxy-15,16,18-trimethyl-13-oxo-14, 39dioxabicyclo nonatriaconta-19,21,23,25,27,29,31-heptene-36-carboxylic acid

Molecular formula: $C_{47}H_{73}NO_{17}$

Molecular weight: 924.09

Chemical structure:

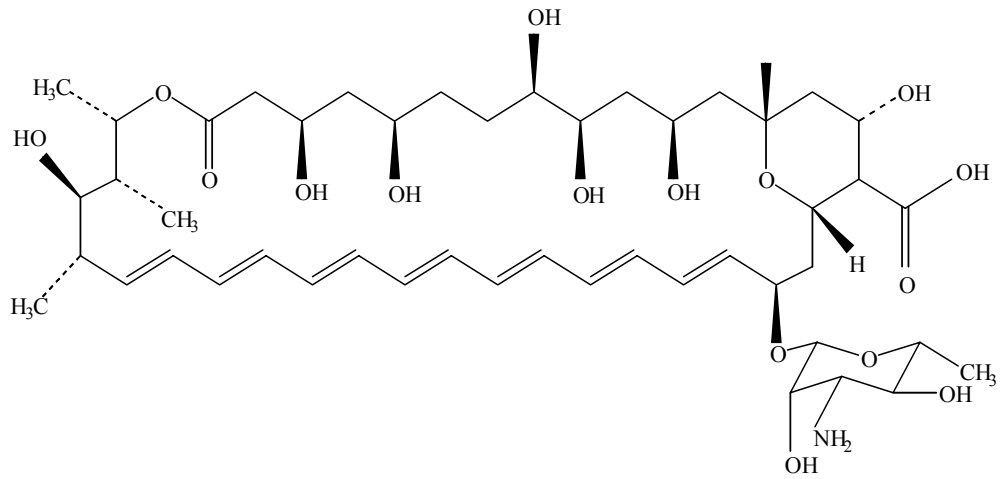

Description: Deep yellow prisms or needle

Boiling point: Decomposes at 170 °C

Solubility: Practically insoluble in water at pH 6 to 7, soluble in water at pH 2 or pH 11 about 0.1 mg/ml, water soluble increased by sodium deoxycholate, alcohol and in ether, slightly soluble in dimethylformamide about 2-4 mg/ml, in dimethylformamide with HCl 60-80 mg/ml and methyl alcohol, soluble in dimethyl sulphoxide and propylene glycol 30-40 mg/ml.

Absorption maximum: The ultraviolet absorption maximum of AmB are 406, 382, 363, 345 nm in methanol.

Stability in solution: The AmB should be kept at 2-8 °C in airtight container and protected from light. Solutions for injection are prepared by reconstitution of AmB with sterile water for injection without preservations to form a colloidal dispersion, which is then diluted with glucose injection. AmB mixed with sodium chloride injection 0.9 % would precipitate the AmB. The pH of the glucose injection should be checked and adjusted with phosphate buffer, if necessary before admixture. AmB solutions should be used immediately after preparation. Although the manufacturer recommends solutions are protected from light, several report indicated that short-term (8-24 h) exposure to light generally does not affect potency.

2. Deoxycholic acid

Synonym: Deoxycholic acid, deoxycholate, desoxycholic acid

Chemical name: (3α, 5β, 12α)-3, 12-dihydroxycholan-24-oic acid or 17β-(1-methyl-3-carboxypropyl) enatio-cholane-3α, 12 diol

Molecular formula: $C_{24}H_{40}O_4$

Molecular weight: 392.58

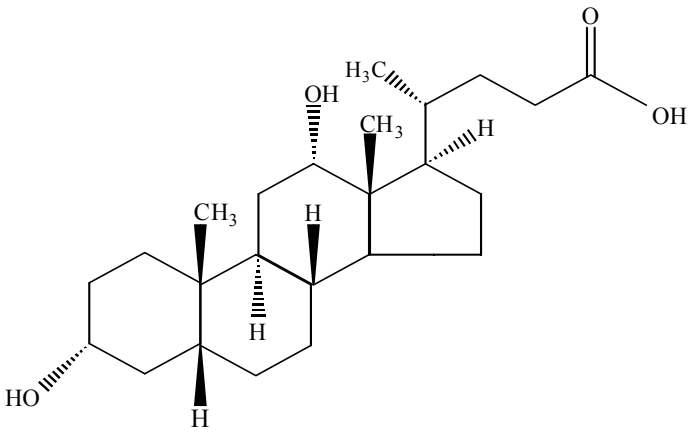

Description: Deoxycholic acid is one of the secondary bile acids, which are metabolic byproducts of intestinal bacteria. The two primary bile acids secreted by the liver are cholic acid and chenodeoxycholic acid. Bacteria metabolize chenodeoxycholic acid into the secondary bile acid lithocholic acid, and they metabolize cholic acid into deoxycholic acid. There are additional secondary bile acids, such as ursodeoxycholic acid. When pure, it comes in a white fluffy to off-white crystalline powder with bitter taste.

Boiling point: 174 - 176 °C

Solubility: Soluble at 15 °C in 0.24 g/l water, in 220.7 g/l alcohol, in 1.16 g/l ether, in 2.94 g/l chloroform, in 0.12 g/l benzene, in 10.46 g/l acetone, in 9.06 g/l glacial acetic acid. Soluble in alkali hydroxides or carbonate, sodium deoxycholate, soluble in water >333 g/l at 15 °C

3. Cholesteryl oleyl carbonate ester

Molecular formula: $C_{46}H_{80}O_3$

Molecular weight: 681.13 g/mol

Chemical structure:

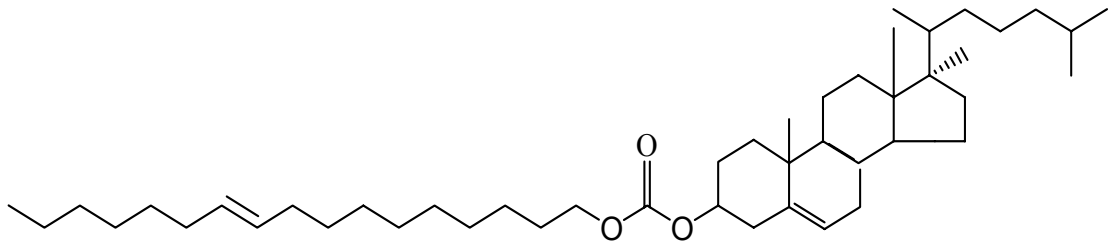

Description: Cholesteryl oleyl carbonate ester is an organic chemical, an carbonate ester of cholesterol and oleyl alcohol with carbonic acid. It is a liquid crystal material forming cholesteric liquid crystals with helical structure. It is a transparent liquid, or a soft crystalline material with melting point around 20 °C. It can be used with cholesteryl nonanoate and cholesteryl benzoate in some thermochromic liquid crystals.The nature of the acyl chain (the chain length and the position and degree of unsaturation) affect the molecular motions of the cholesteryl ester, particularly in the isotropic liquid near the isotropic to liquid crystalline phase transition.

4. Triethylamine

Synonym: N,N –diethylethanamine, N,N,N-Triethylamine, TEA, TEN

Chemical name: N,N –diethylethanamine

Molecular formula: $C_6H_{15}N$

Molecular weight: 101.1 g/mol

Chemical structure:

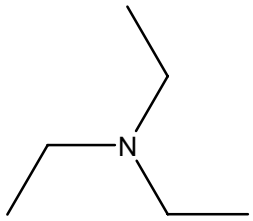

Description: Triethylamine is the chemical compound with the formula $N(CH_2CH_3)_3$, commonly abbreviated Et_3N. It is a commonly encountered in organic synthesis probably because it is the simplest symmetrically trisubstituted amine, i.e. a tertiary amine, that is liquid at room temperature. It possesses a strong fishy odor reminiscent of ammonia. Diisopropylethylamine is a widely used relative of triethylamine. It is also the smell of the hawthorn plant, and semen, among others and commonly employed in organic synthesis as a base, most often in the preparation of esters and amides from acyl chlorides. Such reactions lead to the production of hydrogen chloride which combines with triethylamine to form the salt triethylamine hydrochloride, commonly called triethylammonium chloride.

Density: 0.726 g/cm^3

Melting point: 114.7 °C

Boling point: 89.7 °C

Sublimes: 245 °C

Solubility: slightly soluble in water above 18.7 °C, Incompatible with alcohol, ether, also with water below 18.7 °C, Soluble in 0.7 parts water, soluble in alcohol, chloroform, very slightly soluble in benzene, practically insoluble in ether

Caution: Potential symptoms of overexposure to triethylamine are irritation of eyes, respiratory system and skin.

5. Cetyl alcohol

Synonym: ethal, ethol, palmityl alcohol, alcohol cetylicus, alcool cetilico, cetanol, 1-hexadecanol, hexadecyl alcohol

Chemical name: 1-hexadecanol

Molecular formula: $CH_3(CH_2)_{14}CH_2OH$

Molecular weight: 242.45

Chemical structure:

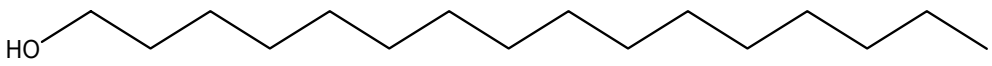

Description: A mixture of solid aliphatic alcohol consisting chiefly cetyl alcohol obtained from spermaceti by saponification. It occurs as white mass, powder, flakes, cubes, or granule with a faint characteristic odour

Melting point: 46-50 °C

Boling point: 344 °C

Density: 0.811

Solubility: Practically insoluble in water, freely to sparingly soluble in alcohol, free soluble in ether, miscible when melted with animal and vegetable oils, liquid paraffin and melted wool fat.

Use: Cetyl alcohol use in topical preparations for its emollient, water absorptive, stiffening and weak emulsifier properties. It may be incorporated into suppositories to raise the melting point and may be used in the coating of delayed released solid dose forms.

6. Cetyl chloroformate

Synonym: Hexadecyl chloroformate

Molecular formula: $C_{17}H_{33}ClO_2$

Molecular weight: 304.90

Chemical structure:

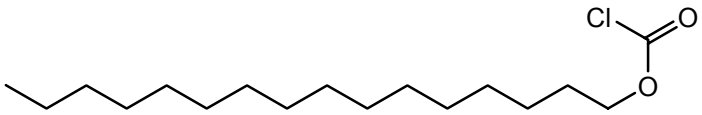

Density: 0.923 g/mL at 25 °C

Refractive index: *n*20/D 1.4480

7. Triphosgene

Synonym: Triphosgene, Bis(trichloromethyl) carbonate

Molecular formula: $C_3Cl_6O_3$

Molecular weight: 297

Chemical structure:

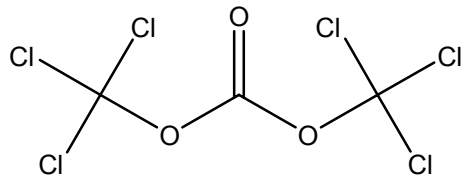

Description: Triphosgene is used as a substitute for phosgene. At room temperature, the compound is a white crystalline solid that decomposes around 130 °C. The decomposition temperature of impure samples is lower. Being solid, even small amounts may weigh easily to add the exact desired amount to a reaction

Density: 4.248 g dm^{-3}

Melting point: 118 °C

Boiling point: 8 °C

VITAE

Name Mr. Sorakom Watcharapinchai

Student ID 4852044

Education Attainment

Degree	Name of Institution	Year of Graduation
Bachelor of Pharmacy	Mahidol university	2001

Scholarship Awards during Enrolment

Acedemic excellence Program in Pharmaceutical Sciences, Prince of Songkla University, 2005-2007

Work-Position and Address

Hospital pharmacist in Chumpuang hospital, Chumpuang, Nakornratchasima 30250, Thailand, 2002-2004

Hospital pharmacist in Padang besar hospital, Sadao, Songkla 90112, Thailand, 2004-2005

List of Publication and Proceedings

Watcharapinchai, S. and Srichana, T. (2007) The effect of synthetic liquid crystals properties Proc.of the 5th Indochina Conference on Pharmaceutical Sciences "Pharmacy for sustainable development". Bangkok, Thailand, 74-80. (Full text proceeding).

Watcharapinchai, S. and Srichana, T. (2007) Effect of synthetic liquid crystals on Amphotericin B properties. Proc.of the 2nd IEEE International Conference on nano/micro engineered and molecular systems. Shanghai, China, 1098-1103. (Full text proceeding).